# COMPUTER CONTROLLED DEVICE TO INDEPENDENTLY CONTROL FLOW WAVEFORM PARAMETERS DURING ORGAN CULTURE AND BIOMECHANCIAL TESTING OF MOUSE CAROTID ARTERIES

A Thesis
Presented to
The Academic Faculty

by

Seth B. Gazes

In Partial Fulfillment
of the Requirements for the Degree
Bioengineering in the
School of Mechanical Engineering

Georgia Institute of Technology
August 2009

# COMPUTER CONTROLLED DEVICE TO INDEPENDENTLY CONTROL FLOW WAVEFORM PARAMETERS DURING ORGAN CULTURE AND BIOMECHANCIAL TESTING OF MOUSE CAROTID ARTERIES

Approved by:

Dr. Rudy Gleason, Advisor (PhD)
School of Mechanical and Biomedical Engineering
*Georgia Institute of Technology*

Dr. Raymond Vito (PhD)
School of Mechanical Engineering
*Georgia Institute of Technology*

Dr. W Robert Taylor (PhD, MD)
School of Medicine, Division of Cardiology
*Emory University*

Date Approved: 6-20-2009

To those that go out of their way to help

# ACKNOWLEDGEMENTS

I would like to thank first and foremost my lab mates who answered countless questions and taught me many skills, whether it be mouse surgeries or MATLAB coding. In particular I would like to thank William Wan and Laura Hansen for the countless times they cannulated arteries for my experiments.

I would like to thank Dr. Robert Taylor and Dr. Raymond Vito for their insightful suggestions and guidance in developing and testing the device. Most deservingly I would like to thank my advisor Dr. Rudy Gleason for his countless support, patience, understanding and insight.

# TABLE OF CONTENTS

# LIST OF FIGURES

## SUMMARY

Understanding the mechanisms of cardiovascular disease progression is essential is developing novel therapies to combat this disease that contributes to 1 in 3 deaths in the United States every year. Endothelial dysfunction and its effects on vessel growth and remodeling are key factors in the progression and localization of atherosclerosis. Much of our understanding in this area has come from in-vivo and in-vitro experiments however perfused organ culture systems provide an alternative approach. Organ culture systems can provide a more controlled mechanical, neural, and hormonal environment compared to in-vivo models. This study focused on furthering development of this organ culture model by introducing a novel device to produce flow waveforms at the high frequencies and low mean flows seen in the mouse model.

First, a number of designs were considered to allow independent control of the amplitude, frequency, shape of the flow waveform. The ability to independently control these parameters results in the independent control of maximum/minimum shear stress and shear rate. The final design incorporated 2 glass syringes driven by a linear motor, while the net positive flow was regulated by 2 solenoid pinch valves. The system was monitored by two pressure transducers, transit time ultrasound flow probe, and a camera. Each individual mechanism in the system was integrated via a computer using Labview.

After designing the system it was then thoroughly characterized. Physiologic, physiologic-oscillatory, low, low-oscillatory waveforms and sinusoidal waveforms were developed using Matlab to produce code necessary to run the motor. This

characterization is not exhaustive but shows the system's ability to modulate frequency, amplitude and waveform independently. Finally, we were able to incorporate the diagnostic capability to measure NO in real-time via and electrical probe. This probe measures changes in current that are proportional to changes in concentration of NO. Attempts were made to characterize Reactive Oxygen Species expression as it relates to flow but no discernable differences were observed with our current confocal microscopy techniques. Overall this system provides a robust model to test the effects of flow on various biological markers both in real-time and after culture.

# CHAPTER 1: BACKGROUND

According the Heart Disease and Stoke Statistics published by the American Heart Association an estimated 80,000,000 American adults (approximately 1 in 3) have some type of cardiovascular disease (CVD)[1]. CVD accounts for one in 2.8 deaths in the United States with total cost on the economy of $475.3 billion [1]. Despite the cost of CVD, both in life and monetarily, the progression of the disease in the arterial system is still not completely understood.

## *General Arterial Structure and Function*

Blood vessels play the essential role of transporting nutrients and waste throughout the body. Arteries transport these nutrients to smaller vessels, arterioles, and capillaries, which service muscles, organs and other tissues. Arterial walls are heterogeneous soft biological tissues composed of endothelial cells, smooth muscle cells (SMC) and extracellular matrix (ECM, Figure 1). The composition of the arterial wall varies significantly along the vascular tree and may be characterized as elastic arteries (e.g., aorta, common carotid, iliac) or muscular arteries (e.g., coronary, femoral, renal).

### Arterial Structure

The arterial wall can be divided in three sections, the intima, the media, and the adventitia. The intima, under normal conditions, consists of a single layer of endothelial cells adhered to a thin layer of sub endothelial connective tissue called the basal lamina. In addition, some arteries (e.g., coronary arteries and aorta) contain a subendothelial layer containing collagen and smooth muscle. The internal elastic lamina is a fenestrated sheet

of elastin that separates the media from the intima. The media consists of smooth muscle cells (SMC), elastin, collagen, and glycosaminoglycans (GAGs). The relative amounts of SMCs and ECM vary along the vascular tree, with an increasing fraction of SMCs in muscular arteries compared to elastic arteries. The adventitia is composed primarily of fibroblasts and Type I collagen, with nerves and vaso vasorum in larger vessels. The thicknesses of the intima, media, and adventitia also vary with location along the vascular tree; for example, the ratio of media to adventitia thickness in common carotid arteries is large compared to that in coronary arteries. A more comprehensive review may be found in Rhodin, 1979 and Humphrey, 2002[2].

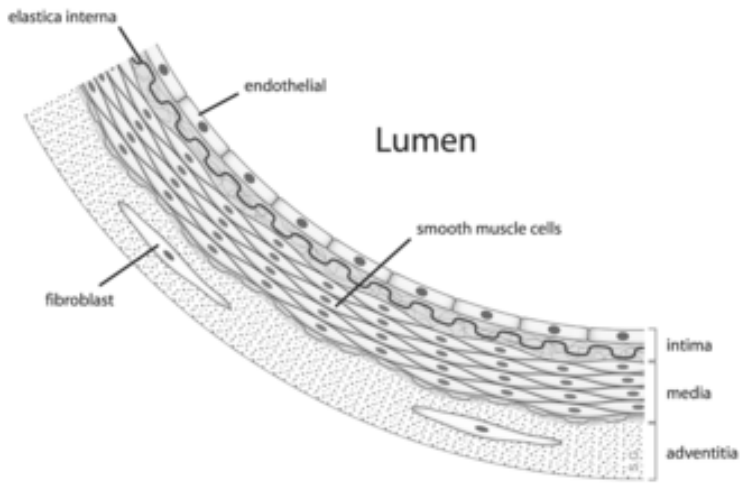


**Figure 1 - Arterial Layers**

## Mechanical Environment

Arteries are exposed to multiaxial mechanical loads, including (a pulsatile) blood pressure that causes the vessel to cyclically distend circumferentially, blood flow that induces a shearing load along the luminal surface, and an axial extending load; the latter is relieved upon excision, causing the vessel to retract. The heart ejects and fills with

blood in alternating cycles of systole and diastole, creating a cyclic pumping that results in unsteady pulsatile flow and pressure in the arteries [3]. In most cases, blood flow in arteries remains forward or zero; however, during diastole, flow rates can become reversed in many locations along the vascular tree (i.e. carotid sinus, external carotid, brachial, and femoral arteries). In general, the mean pressure and the magnitude of pulse pressure decrease with distance away from the heart, with a significant drop in mean and pulse pressure across arterioles[3].

Arteries exhibit a non-linear stress-strain response; they exhibit a visco-elastic response, and, they are heterogeneous, orthotropic, and nearly incompressible[2]. Under physiological loading arteries experience large deformations, with circumferential and axial strains components on the order of 0.3-0.9. Each component of the artery wall plays a different role in response to these deformations. Elastin is more compliant than the other components of the media. It also releases and stores energy over a large range of deformations. Collagen is crimped when unloaded and bears greater mechanical loads as the deformations increase. SMCs come in two forms, contractile and synthetic. Synthetic SMCs produce parts of the ECM and Contractile SMCs play an active contractile mechanical role. Normally SMCs are partially contracted giving the vessel a basal muscle tone. However stimuli such as altered flow or pressure will cause SMCs to contract or dilate. When SMC's contract they have a larger mechanical contribution in the vessel. This mechanical contribution of the SMC's with respect to ECM is not uniform in all arteries and varies depending on the location along the vascular tree. SMCs play a greater mechanical role in muscular arteries that need to constrict and dilate often to regulate blood flow to an organ or other tissue[2]. This is true for mesenteric

arterioles that regulate blood flow to the intestines and therefore have a high level of basal muscle tone. The adventitia plays a mechanical role at high pressures as it is thought to reinforce the structural components of the media that lie internally.

The ratio of collagen, elastin, and GAGs vary depending on the size and location of the artery. In a healthy mature artery there is a homeostasis between cell proliferation and cell death, as well as extracellular-matrix synthesis and degradation. Synthetic SMCs play a role in ECM maintenance by producing elastin and collagen while matrix metalloproteinase are involved in ECM degradation. This balance or homeostasis maintains healthy arterial structure, geometry, and composition. However, aging and disease can cause changes in the ratio and organization of vascular tissue as well as its overall arterial mass.

## *Arterial Growth and Remodeling*

Growth, as define by Humphrey[2]," is an increase in mass achieved via an increase in the number(e.g. proliferation, hyperplasia, or migration) or size(hypertrophy) or cells and/or synthesis of extracellular matrix that exceed degradation". Remodeling can be defined "as a change in internal structure that is achieved either by reorganizing existing constituents or by synthesizing new constituents that have a different organization"[2]. Therefore remodeling results in a change in material properties due to changes in the mechanical environment.

The mechanical environment in which an artery lives can be described using both global (blood pressure, flow rate, and axial force) and local (circumferential stress, shear stress, and axial stress) hemodynamic parameters. The mechanical environment of cells is considered local because circumferential stress, shear stress, and axial stress are felt by

cells. The mechanical environment of vessels is considered global, because pressure, flow rate, and axial force act on the vessel as a whole (this sentence is a little confusing). This mechanical environment is a key driver of remodeling. These local and global parameters are related to each other using force equilibrium and flow equations below.

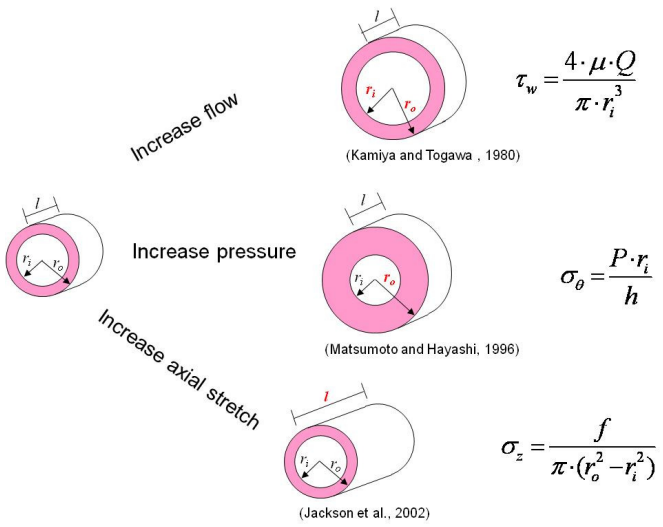


**Figure 2 - Three basic mechanisms of arterial remodeling**

Changes to an artery's local parameters such as circumferential stress, flow induced shear stress, and axial stress alter the homeostasis of the vessel. To restore natural homeostatic levels, the artery remodels itself in a way that maintains stresses felt by the cells that make up the vasculature. The response required differs for each parameter type. When pressure increases in the artery, an increase of the artery's outer radius results and while the inner radius remains constant so that the cells can feel their normal mechanical environment. When flow increases, luminal area increases via an increase in the inner radius. Additionally a secondary effect of the luminal diameter increasing is an increase in the hoop stress; therefore the vessel wall thickens to return the wall stress to homeostatic level. When sheer stress increases, the endothelial cells up-regulate

vasodilators that relax the smooth muscle cells, increasing the diameter of the vessel [4-6]. The artery is therefore an adaptable organ that changes depending on its mechanical environment, always attempting to restore basal level homeostatic values of circumferential stress, axial stress, and shear stress. Although these adaptations are meant to protect the vessel in the short term over time these adaptations can manifest themselves as disease.

### *Wall Shear Stress and Arterial Disease*

An increase in flow rate can cause an artery to dilate via a temporary relaxation of the SMCs followed by a long term reconstruction of the media. The long term reconstruction involves the proliferation and migration of SMCs that increases the diameter of vessel to restore homeostatic values of shear stress[7]. The opposite is also true for a decrease in flow although the mechanism to restore shear stress is different. At first SMCs contract due to the release of vasodilators and endothelium-derived relaxing factor (EDRF) by the endothelium. If the low flow (shear) conditions are chronic the process will continue with the vessel mostly thickening in the intima in order to restore the shear stress. Reductions in the release of EDRF or an increase in the concentration of vasoconstrictors may be mediators of this process. If remodeling is not able to change the geometry sufficiently to achieve the homeostatic shear stress, continued cell proliferation and growth can occur leading to arterial disease.

### Hemodynamic Factors

While disease states such as high blood pressure can alter an artery's local hemodynamic parameters, the vessel's geometry itself causes changes in these parameters which can lead to arterial disease. The curvature and branching of the carotid

bifurcation causes areas of low and oscillating wall shear stress (and flow). These areas show intimal thickening and, subsequently, atherosclerotic plaque formation. However areas of low wall shear coincide with areas of oscillating flow, making it difficult to separate correlations between low and oscillatory wall shear stress and intimal thickening [8-10].

## Disease Progression

While these hemodynamic factors appear to localize atherosclerosis, the likelihood of progression from intimal thickening to atheroma involves a number of factors. These include, but are not limited to, cholesterol levels, smoking, diabetes, and hypertension. These factors increase the likelihood of injury to the endothelial layer of the vessel. Once this occurs dysfunction develops and increases permeability the following cascade of events results. Monocyte adhesion to the endothelium and emigration into the intima begin to take place. Smooth muscles then emigrate from the media to the intima, and the monocytes that have permeated the membrane develop into macrophages and then into foam cells. These macrophages and smooth muscle cells engulf lipids that have entered the intima in response to the increased permeability. Smooth muscle cells proliferate in the intima and the extracellular matrix begins to reconstitute itself around the lipid debris, forming the atherosclerotic plaque[11].

## Biologic Markers

Monocyctes and macrophages play a key role in atherosclerosis. These cells adhere to the endothelium and have specific cell surface binding proteins for the surfaces of dysfunctional endothelial cells (EC). Once bound to the EC the monocytes extravasate into the intima where they transform into macrophages and engulf lipids eventually

$$NAD(P)H + 2O_2 \rightarrow NAD(P)^+ + H^+ + 2O_2^{\cdot -}$$

becoming the foam cells which make up the lipid core of atherosclerotic lesions. Monocytes are originally attracted by MCP-1(Monocyte Chemo attractant Protein-1) and their rolling and adhesions to the vessel wall are modulated by E-selectin and VCAM-1 (Vascular Cell Adhesion Molecule-1). Once located within the intima, macrophages produce a number of products including additional MCP-1, which recruits more monocytes to the area, TNFα(tumor necrosis factor alpha), which further induces the inflammatory response, IL-1(interleukin-1), which increases the expression of adhesion factors on endothelial cells, and the production of reactive oxygen species (ROS) such as superoxide and hydrogen peroxide. These ROS mediate the inflammatory response through up regulation of pro-inflammatory genes. Several enzymatic reactions produce these ROS, but the most common source is NADPH Oxidase. The majority of ROS produced in vessels walls are produced in smooth muscle cells and fibroblasts[12].

Under normal conditions Nitric Oxide(NO) is an important atheroprotective molecule. Vascular NO dilates blood vessels by stimulating guanylyl cyclase and increasing cyclic guanosine monophosphate (cGMP) in smooth muscle cells. NO release in the lumen inhibits platelet aggregation and adhesions as well as leukocyte adhesions. Since white blood cell adhesion is one of the critical events in the onset atherogenesis, this may be a mechanism of NO's atheroprotective nature. Additionally, NO has been shown to inhibit the proliferations of smoothe muscle cells, a later step in atherogenesis[13].

Most vascular production of NO is due to endothelial NO synthase (eNOS) . In its normal state eNOS oxidizes its substrate l-arginine to l-citruline and NO. This functionality requires dimerization of the enzyme, the substrate of L-arginine, and an

important cofactor (6*R*)-5,6,7,8-tetrahydro-L-biopterin ($BH_4$). Due to NO's atheroprotective nature, it may appear that an increase in eNOS expression, which would therefore lead to an increase in NO production, could decrease the risk of atherochlerosis. However, in actuality, cardiovascular risk factors are *increased* with an increase in eNOS expression[13].

This is because in the presence of oxidative stress or ROS, NO can become atherogenerative. Most vacsculature produc tion of NO is derived from endothelial NO synthase (ENOS). In its normal state eNOS oxidizes its substrate l-arginine to l-sitruline and NO. In the presence of ROS, in particular superoxide ($O_2^-$), NO reacts with peroxynitrite iand the atheroprotective nature of NO decreases. Additionally eNOS begins to make peroxynitrite ( $ONOO^-$) instead of NO, eventually becoming an enzyme that generates solely $O_2^-$.[10] One of the products of the dismutation of $O_2^-$ is $H_2O_2$.

$2O_2^- + 2H^+ \rightarrow H_2O_2 + O_2$

$H_2O_2$ has been shown to increase eNOS expression through transcription and posttranscription mechanisms[14]. However, although there is an upregulation of eNOS, it is enzymatically disfuncitonal in the presenece of oxidative stress and begins to generate $O_2^-$ instead of NO.

## *Organ and Tissue Culture Devices*

In-vivo investigations provide conditions that are physiologic but it is difficult to monitor precisely and continuously the mechanical environment and remodeling response of arteries. Additionally many factors, including hormonal and metabolic changes, may affect smooth muscle cell activity and remodeling. Organ and tissue culture devices provide a unique method to keep the vessel in a well-defined biochemical environment

that isolates the vessel from non mechanical factors. This type of device is ideal for determining the effects of the mechanical environment on the organ or tissue. Because remodeling in response to altered flow takes longer that current organ culture devices can keep smooth muscle cells viable, most investigations to date have explored growth and remodeling in response to changes in pressure.

Many devices have been developed to both test and/or culture vascular cells and tissues. Arterial cells are subjected to both fluid shear stress due to blood flow and cyclic hoop stress due to pulse pressures during the cardiac cycle. The ideal testing device should be able to vary both blood flow and pulse pressure at the physiological frequencies and ranges of the vessel tested. A comprehensive device must also be able to independently vary blood flow and pulse pressure under varying disease conditions; i.e. high and low blood pressure, oscillatory, low wall, and high wall shear stress.

Some recent tissue culture systems have developed bioreactors for the tissue engineering of vascular grafts. Abiliez et al. [15]have designed a device to culture undifferentiated mouse embryonic stem cells in a three dimensional configuration under physiologic pulsatile flow and pressure conditions. This device incorporates pressure transducers before and after the culture chamber, an outlet flow probe, a data acquisition system, and a flow probe. However, this system did not measure flow at the point of interest, in this case the culture chamber, nor produce murine physiologic maximum flow rates of 2.5 ml/min. The device was able to produce the pulsatile flow rate and pulse pressure at 10 hz; but the flow profile resembled a sinusoidal waveform rather than the 1/3 – 2/3 physiologic waveform that has higher shear rates.

Gleason et al[16] developed a device that shared many qualities with Abiliez et al's, although it was originally designed for organ culture and biomechanical testing of mouse arteries instead of tissue engineering, although most recently it has been used for tissue culture…. It produces the physiologic pulse pressures at 10 hz. Although mean flow can be controlled in physiologic of 0-10 ml/min; the shape of the flow waveform cannot be controlled to model oscillatory, low wall, and high wall shear stress. This device can measure axial load, pressure, as well as diameter and control axial stretch as well as transmural pressure.

Peng et al[17] created a device which uses a flow pump and linear servo-motor pump in series to produce a mean flow-rate and pulse pressure. A PID controller is used to control the mean flow rate and the amplitude and waveform of the pulse pressure. However this system is not able to produce physiological flow profiles at low flow rates (or low wall shear stress), an important flow condition to study the biomechanical and biological response of disease progression in arteries. Additionally the PID controller only acted on pressure data, therefore tuning of the flow waveform was secondary and only a result of changes in mean flow rate and pulse pressure. The waveforms at low and high flow rates did not appear to have physiologic shear rates or waveforms. Particularly, at lower flow rates (10ml/min), flow reversal is observed as pulsatility increases although this cannot be controlled independently.

Moore et al's [18] device decouples the effects of shear stress (flow) and hoop stretch (pressure) on endothelial cells seeded on tubes, by fixing the seeded tubes with non compliant sleeves to prevent cyclic hoop stretch. With this setup, four conditions can be studied (1) static (no shear stress or hoop stretch) (2) shear stress only (with sleeve) (3)

hoop stretch (low flow and no sleeve), (4) shear stress and hoop stretch (normal flow and no sleeve). Although robust in its ability to compare simpler cases of (2) and (3) to the static conditions of (1) and complex conditions of (4), the system is not appropriate for murine vessel culture because of its inability to produce pulse frequencies of 10 Hz. Additionally, disease conditions cannot be studied because the system is unable to reverse flow to cause a disturbed flow environment.

# CHAPTER 2: OBJECTIVES

Despite significant advances in the development of cell culture devices there are still questions regarding the single contribution of each component of blood flow; mean flow, amplitude, and frequency. To do this, a system must produce a variety of flow waveforms (physiologic, high, low, oscillatory) at various frequencies up to 10Hz[19]. This type of system allows for the study of the contributions of the different harmonics flow (mean flow, amplitude, and frequency) on growth and remodeling. Additionally this type of system can also be used to determine therapeutic effects of mean flow, amplitude, and frequency on vessels in culture.

The design of comprehensive organ culture device that can produce both physiologic and disease state flow waveforms is important for the study of cardiovascular disease in the murine model. The ability to decouple low wall shear stress from oscillatory wall shear stress while studying vessels in culture is a good model not only to determine how each of these conditions affects the biomechanics of the vessel but also to determine if there is a difference in the NO or ROS response under oscillatory, low wall shear stress, or both. Towards this end, we have completed the following specific aims,

**Specific Aim 1: Design a device that produces continuous flow at various waveforms and physiologic frequencies for use in mouse vessel culture systems.**

Previous organ and cell culture devices have not been shown the ability to control the flow waveform at high frequencies to produce oscillatory, low wall, and high wall shear stress [15-18] in mouse vessels. A number of different designs were considered including a simple pulsating valve in series with a compliance chamber. Eventually an

adaptation of the device used in Conway et al [20] was chosen because its performance to produce oscillatory flow at 1 Hz had been observed in a parallel plate flow chamber. A detail design followed using a series of three way valves, two syringes mounted on a linear motor, and an ultrasound flow meter integrated in LABVIEW 7.0 (National Instruments).

**Specific Aim 2: Characterize the device capabilities to produce low wall, high wall, oscillatory, and physiologic shear stress in mouse vessels at frequencies of 1, 5, and 10 Hz.**

Flow was measured using a Doppler ultrasound system mounted over the vessel or calibration tubing. More detailed development of syringe mounts was necessary to get identical motion responses between the motor and the syringes driving the fluid. Additional tuning of the PID controller of the motor was necessary to achieve the high frequency response that produced high wall, low wall, oscillatory, and physiologic shear stresses at 10 Hz. Sine waveforms as well as the 1/3-2/3 physiologic waveforms were produced in to study affect of shear rates on cultured vessels.

**Specific Aim 3: Incorporate diagnostic capability to measure NO in real time and quantify levels of ROS in live vessels after culture under various flow waveforms.**

Vessels were subjected to vasodilators and constrictors after culture to determine smooth muscle cell viability after culture with the device. NO was monitored during vessel culture while maintaining frequency but changing the waveform and vice versa. A fluorescent ROS probe was utilized to determine if culturing with this device decreases the amount of ROS in the vessel.

# CHAPTER 3: METHODS

A robust drive mechanism and secondary flow loop was designed in order to produce a number of different flow waveforms at various frequencies. This device can be used in conjunction with the multiaxial organ culture and biomechanical testing device used in Gleason et al[16] or various off the shelf testing vessel testing devices.

## *Experimental Set-up*

### Design Concept

Many designs were considered to produce the various flow waveforms at frequencies up to 10 Hz. The first design considered was a single syringe mounted on the linear motor with a solenoid valve and vessel downstream and the reservoir upstream (Figure 3). This design most resembles the physiology of the cardiovascular system. The oscillation of the syringe mounted to the linear motor both drives media out through the vessel. During diastole or pull phase media is drawn into the same syringe. This is similar to the biomechanics of the heart pushing blood out during systole and pulling blood from the lungs during diastole. However in this design the motor needs to move forward and reverse very small increments at a very high frequency. Additionally the valve needs to open and close at this same frequency and in synchronization with the high frequency oscillating movements of the linear motor. Reading the encoder position and engaging the solenoid valves at the in this time frame through LABVIEW proved difficult considering each loop in the LABVIEW program took 50 ms to execute while the response time of the solenoid valves was 25 ms. Additionally the production of a

custom glass syringe with two ports, one accessing the reservoir and the other to the vessel, proved difficult in the glass shop.

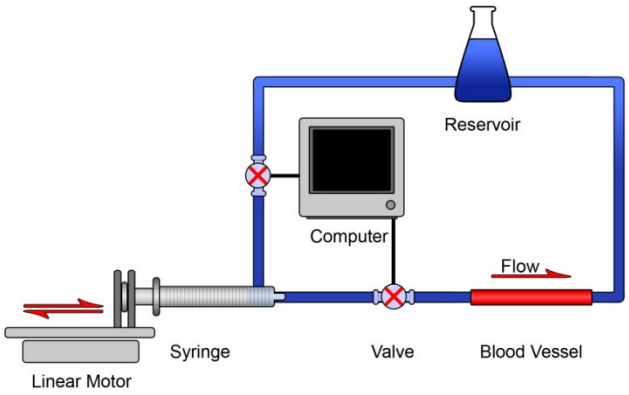


**Figure 3 - Design 1 integrated a syringe mounted to a computer controlled linear motor and two computer controlled solenoid valve. The syringe would pulse the desired waveform, followed by the simultaneous closing of the valve proximal to the vessel and opening of the valve between the syringe and reservoir. At this time the syringe would recharge with liquid during the zero flow portion of the profile. Labview was used to control all three, although syncing the two valves and motor movements at 10 Hz proved difficult.**

Another design considered was peristaltic pump in series with a capacitance chamber and a solenoid valve proximal to an organ culture device (figure 4). The flow waveform observed is shown below and presents this design's modularity with respect to frequency. The system was able to produce a waveform at 10 Hz. However the system was not capable of changing to waveform to produce higher, lower, or oscillatory shear stresses.

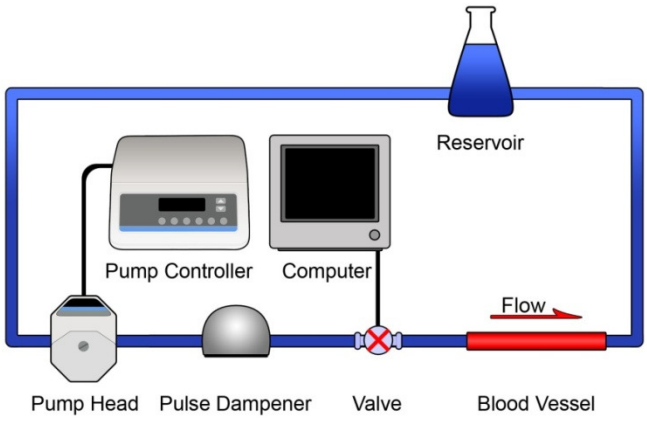


**Figure 4 - Design 2 incorporated a solenoid valve, pulse dampener, and pump head all proximal to the vessel chamber. The pump was set the desired mean flow rate independently of the computer. The valve was computer controlled and opened and closes at frequencies up to 10 Hz. The silicon tubing proximal to the valve served as a capacitance chamber that would enlarge and store liquid while the valve until the valve opened. This capacitance gives the device its capability to deliver a low flow pulsatile waveform.**

The final design consisted two 1 mL glass syringes (VWR) mounted in opposite directions on a linear motor (MX80L, Parker Motion) using CNC machined syringe mounts. The syringes were connected to the vessel culture device (Living Systems) using a series of three-way Luer lock valves (Cole Palmer) and Masterflex PharMed L/S-13 tubing (Cole Palmer). L/S-13 tubing is relatively rigid, has a small diameter, thick walls and was chosen to reduce the capacitance in the system. This tubing is connected to each other and various glassware using luer lock fittings (Cole Palmer).

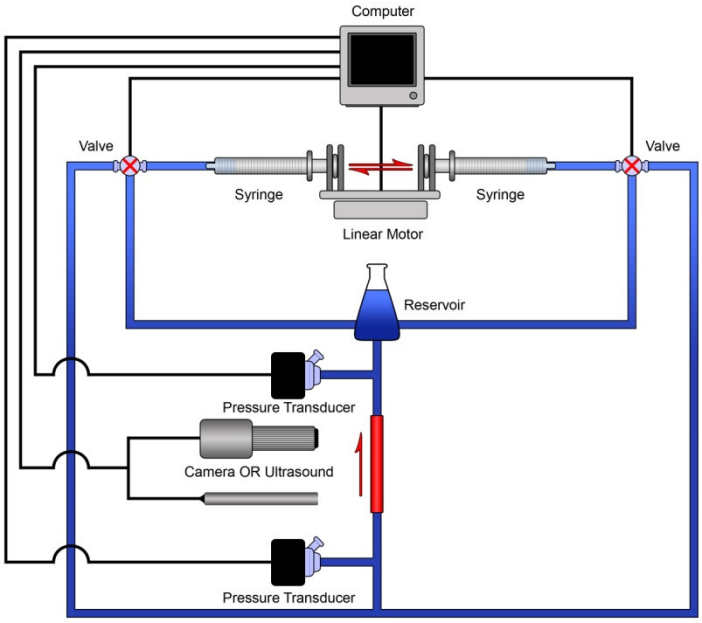


**Figure 5 - Final Design integrated the linear motor, transit time ultrasound, camera, two pressure transducers, and two valves. All of these peripheral devices are controlled with the same Labview program. Continuous flow was maintained by the synchronization of the valves; when a syringe is drawing liquid the valve is open to the reservoir and when the syringe in pushing the corresponding valve in open to the vessel.**

As motor moves from right to left the syringe on the right pushes out media with a prescribed waveform through the tubing and valve into the Living Systems device. During this same time period the syringe on the left pulls fluid from the reservoir into the chamber. When the linear motor reached a designated encoder count both valves switch their positions, the right one opens to the reservoir and the left one opens to the vessel, and the platform on the linear motor reverses direction but maintain the same waveform. The simultaneous switching of both valves and reversing of direction enables continuous flow with the commanded waveform.

## Motor Set-up

The motor selected (MX80L, Parker Motion) is able to make rapid accurate movements but does not have the torque limits of other types of linear drive mechanisms, e.g. induction motor with gear head and lead screw. However our priority requirements are small accurate movement and therefore we had to sacrifice maximum torque when selected this motor. We compensated for this by reducing friction in the system. The motor set-up consisted of the motor, motor controller (ACR 9000), motor driver, and power supply.

The motion of the motor was controlled using spline code in which a series of time points and X coordinates are uploaded to the motor controller. Matlab was used to produce the lines of spline code that correspond to the flow waveform desired (see Appendix 1). These points are coded into a program that is uploaded to the motor controller. When the program is run the motor moves to the commanded X-coordinate at the designated time point K. An example of this code is show below in figure 6. Once uploaded, to code is run via a Labview program that communicates directly with the motor controller.

```
k 0.000 x -0.000
k 0.040 x -0.039
k 0.080 x -0.000
k 0.120 x -0.000
k 0.160 x -0.000
k 0.200 x -0.079
k 0.240 x -0.118
k 0.280 x -0.079
k 0.320 x -0.079
k 0.360 x -0.079
k 0.400 x -0.157
k 0.440 x -0.196
```

**Figure 6 - Example spline code produced using Matlab and uploaded to motor controller. K represents each time point and X represents the position along that axis of the motor**

Using Labview to control the motor instead of the Parker propriety ACRview program allows for easy integration of motor information, i.e. encoder position, with the

response of other entities in the system, i.e. valve control and flow detection. In order to improve motor performance by decreasing the lagging error over time the spline code was slightly modified so that the motor would have programmed stops of 250ms at its minimum and maximum x-position. This allows for the motor regularly home during extended culture and in doing so reducing any lagging error that aggregates in the PID controller overtime. Additionally because each loop of the Labview program take at minimum 50 ms to execute this assures that any external operations that occur at the maximum and minimum x-positions of the motor don't miss the corresponding encoder position.

## Drive Mechanism

The drive mechanism of the system consists of the motor (discussed above), the syringe, syringe mounts, and the mounting plate. The glass 1 ml syringes translated the displacement of the motor to displacement of liquid with low levels of friction compared to plastic syringes. Although the air does not penetrate the precision fit of the glass syringe's plunger and chamber over a few draw/inject cycles, this is not true over 1000 cycles where air bubbles are apparent.

Four syringe mounts (two for each syringe) were machined on a CNC mill to assure precise alignment between the chamber and plunger of both syringes and the linear motor driving the motion. Grooves were milled out of the chamber mounts so that the syringe rested at the correct height and along the midline of the mounting plate. The plunger tightening plates were designed to align the plunger along the center line as well provide a tight coupling between the motion of the syringe and the displacement of the

motor. The chamber tightening plates were designed to reduce chamber displacement along the centerline during the inject/draw cycles of each syringe.

The mounting plate was designed to integrate the linear motor, syringes, and syringe mounts along the same centerline. This plate was machined out of PVC for easy cleaning and provides a mounting surface for attaching the two chamber mounts and the linear motor.

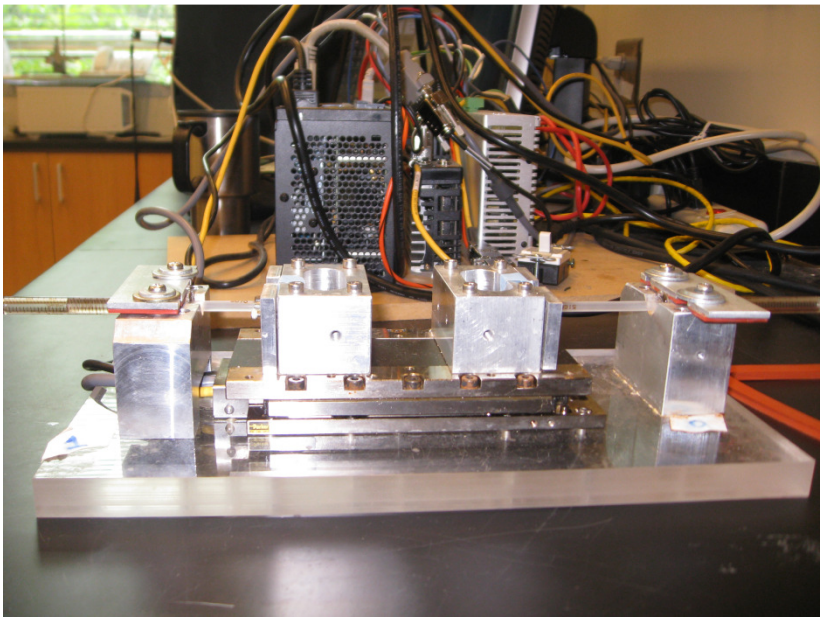

**Figure 7 - Drive Mechanism**

## Flow Loop

In the confined space of an incubator the layout of tubing is important to maintain consistency of flow waveform between groups and reduce compliance in the system. Masterflex PharMed PBT L/S-13 tubing was used throughout the system because of its relatively large wall thickness. PBT L/S-13 tubing provided a nice compromise between the flexibility and compliance of silicon tubing and the rigidity of PTFE tubing. Tubing was connecting using 1/16" Luer lock fittings throughout the loop.

Priming the system is important to purge the flow tubing and connections of air. This improves the response of flow with regard to the displacement of the syringe by making the liquid more incompressible. Two 10 ml glass syringes connected to the three-way valve at on each 1ml syringe is used to first prime the lines that service the reservoir. Secondly the each valve is switched and lines to the living system device are primed.

## Valve Control

Three-way solenoid pinch valves (Cole Parmer EW-98302-40) were used to control flow between the syringe, reservoir, and the vessel. These valves control the flow of fluid without coming in direct contact with the fluid which reduces contamination and eases sterilization. The tubing is silicone based and has and ID of 1/32", similar to the ID of the rest of the tubing in the flow loop. The tubing in the valves was shortened in order to reduce compliance in the system.

The same labview program used to control the motor was also used to control the valves because there opening and closing of them depends on encoder position. The valves have a fast response time of 25 ms therefore any lag in the system is due to computing time in the Labview program used to control the valves. The Labview loop execution time was at least 50 ms and over time could increase to 200 ms, therefore programmed 250ms stops at the motors maximum and minimum position assure the respective encoder value is satisfied for the valves to open or close. Additionally the digital outputs of the National Instrument DAQ can only output a maximum of 10 V while the valve energizes at 12 VDC. Therefore the valves must be powered from an external power source but controlled via the DAQ and labview. To regulate the power

source a circuit, consisting of transistor and a flywheel diode, was designed and built to serve as a switch. When the transistor is energized with 5 V the gateway opens allowing current to flow producing the 12 VDC necessary to activate the solenoid (Figure 8).

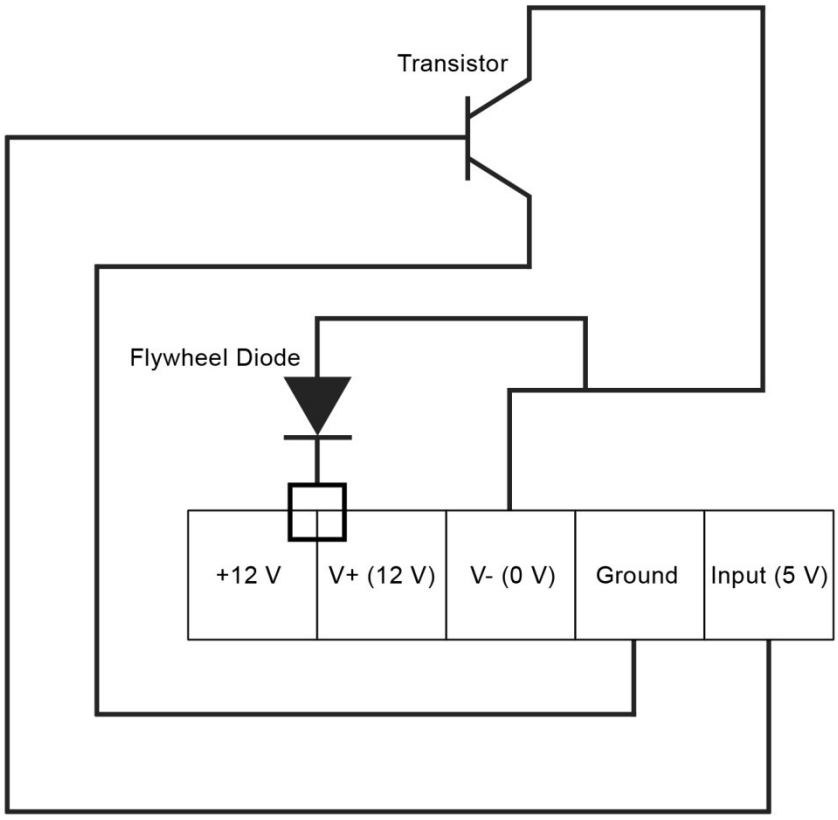


**Figure 8 - Solenoid Valve Circuit**

## Flow Detection

In order to detect flow in the through the carotid artery a Transit Time Doppler ultrasound system from Transonic Systems was utilized. The system consisted of .7PS probe with a resolution of .05 ml/min, zero offset of +- .2 ml/min, absolute accuracy of +- 15%, and an ultrasound frequency 9.6 MHz. A Transonic TS420 Flow Meter Module

was used to measure the signal from the probe. The module has a maximum bandwidth of 160 Hz to accurately measure flow dynamics of high frequency heart rates.

Time Transit Doppler ultrasound sound probe consists of a probe body that houses the two ultrasound transducers and fixed acoustic reflector opposite the probe body. The flow meter measures both the upstream transit time and downstream transit time via the probe. To measure the upstream transit time the downstream transducer emits a plane ultrasound wave that bounces off the reflector onto the downstream transducer. To measure the downstream transit time the transmitting and receiving functions of the two transducers is reversed and the ultrasound sound wave travels in the opposite directions. The flowmeter subtracts the upstream and downstream transit times which is then integrated to determine volumetric flow rate.

The difference between the downstream and upstream transit time is calculated by the flow meter using wide beam ultrasonic illumination. One ray of an ultrasonic beam undergoes a phase shift in transit time that is proportional to the average velocity of the liquid times the path over which the velocity is encountered. The receiving transducers some these velocities; whereas the average velocity multiplied by the vessel's cross sectional area yields volume flow.

## *System Characterization*

The system was characterized using with Pebax tubing (.5 mm OD) canulated on the living systems device and secured using a silicone based adhesive. The system was set up inside of an incubator at 37 °C with the atmosphere maintained at 5% $CO_2$. The design and flow loop were set-up as show in the previous section. The reservoir was pressurized at 100 mmhg using a flow restricting pressure controller (Alicat Scientific).

### Frequency

Physiologic waveform were developed using Matlab then uploaded to the motor controller and finally the flow data was then analyzed with Matlab to determine the actual flow profile of the liquid through the calibration tubing. Testing waveforms were developed at 1 Hz, 5 Hz, and 10 Hz in order to test the vessel response to changes in shear rates when max and mean shear stress remains the same.

### Flow Profile

In addition to developing waveforms at various frequencies, waveforms were developed at different profiles at each frequency (1 Hz, 5 Hz, 10 Hz). Five different waveforms were developed; the physiologic waveform with max flow rates of approximately 2.0 ml/min and a mean flow rate of .7 ml/min, the physiologic oscillatory waveform with max flow rate of 2.0 ml/min but with an oscillatory component that lowered the mean flow rate, the low flow waveform with a max flow rate of 1.0 ml/min, and low flow oscillatory waveform with a max flow rate of 1.0 ml/min but with an oscillatory component that lowers the mean flow, and a high flow waveform with a max flow rate of 3.0 ml/min.

## *Biological Measurements*

In order to validate the functionality of the device two different tests were performed to characterize the biological changes that occurred in the vessel during testing. Two tests were also performed to determine cell viability, smooth muscle cell, and endothelial cell functionality after testing.

## Surgical Preparation and Aseptic Set-up

All system components that contact either the vessel or media were sterilized using an ethylene oxide sterilizer for 12 hours. Surgery and system assembly were performed in a laminar flow hood. Mounting of the syringes to the motor mounts were performed in the incubator once all flow loop connections were made.

Wild-type adult make mice (Jackson Laboratories) were anesthetized with sodium pentobarbital (100mg/kg IP). Both carotid arteries were isolated, placed in fresh culture media, dissected free of perivascular tissue, and mounted on the cannulae using sterile 7-0 suture. The vessel was bathed and perfused with Dulbecco's Modified Eagle medium(P/S Invitrogen, Inc ) antibiotics (1000 units/L of penicillin and 100 g/L of streptomycin), and 0% to 20% heat activated bovine serum (HI-FBS, Hyclone). Usually carotid arteries were excised and introduced in the flow environment within 1 hour.

## Functional Testing

A Methyliazol tetrazolium(MTT) assay was used to determine general cell viability after 6 hours of culture under physiologic waveform at 10 Hz. The MTS assay measures the activity of the reductase enzyme that reduces MTT to formazan resulting in a purple color, and therefore measures the metabolic activity of cells. Following the culture carotid segments were incubated for 1-2 hours in an incubator at 37 °C. Pictures were taken of the entire carotid segment using a digital camera after incubation in the MTT was complete.

Contractile function of the vessel was determined at prescribed time points by observing the relative changes in diameter in response to the subsequent administration of three agents to the adventitial bath: Phenylephrine (PE) to elicit smooth muscle cell

contraction, acetylcholine (Ach) to elicit endothelial-dependent dilation, and sodium nitropruside (SNP) to elicit endothelial-independent dilation.

## Nitric Oxide Sensor

Levels of NO release into the lumen were determined using a 200 µm probe (World Precision Instrument) and an Apollo 1000 data acquisition system (World Precision Instruments). The vessels measured NO levels 3 cm distal to the vessel at the 3-way valve. NO levels were measures using Data Trax software integrated into the data acquisition system. The probe has a response time of <5 msec, minimum detection limit of .2nM, and a sensitivity of 10 pA/nM.

NO detection was recorded after immediately after excising the vessel. The vessel was held in a zero flow environment, then subjecting to physiologic flow for 20 minutes, and finally cessation of flow.

## Reactive Oxygen Species Probe

The presence of reactive oxygen species was measure using a hydrocyanine3 probe developed specifically for the detection of ROS[21]. The HCy3 probe excites at 535 λ and emits at 560 λ when using confocal microscopy. The probe was introduced after 1mg of hydro-Cy3 probe was diluted in 1 mL of methanol. Then 500 µl of the HCy3 methanol stock is further diluted into 100 ml of phosphate buffered saline (PBS). Then the lumen of the vessel was perfused (.7 ml/min) with PBS for 5 min using a Masterflex peristaltic pump connected to the living systems device that contains the cannulated vessel. The vessel is then perfused in a similar manner with the HCy3-methanol-PBS solution for 10 min at a lower flow rate of .2 ml/min. Then the vessel is perfused with

PBS again for 2 minutes in order to rinse the lumen of any residual probe. The vessel is then perfused with 10% formalin in order to fix the cells. A positive control vessel was Two flow conditions were tested in order to determine the level of ROS expression. The vessel was tested with the probe after a low flow culture (.20 ml/min) and physiologic flow culture (.7 ml/min at 10 Hz) after 6 hours. Images were taken both before introduction of the probe and after using Zeiss LSM 540 confocal microscope.

# CHAPTER 4: RESULTS AND DISCUSSION

Experiments were conducted to define the novel device's ability to produce various physiologic and disease waveforms at frequencies from 1 – 10 Hz. Additionally we incorporated a probe to measure NO release during culture was performed and methods to introduce an imaging probe for ROS production, which can be imaged via confocal microscopy of the vessel while still mounted on the organ culture device.

## *System Performance*

Mouse in vivo flow measurements of the carotid artery of an anestitized mouse using Doppler ultrasound show a mean flow rate of 1 ml/min. Minimum flow is measure at .6 ml/min and max flow is measured at 2 ml/min.

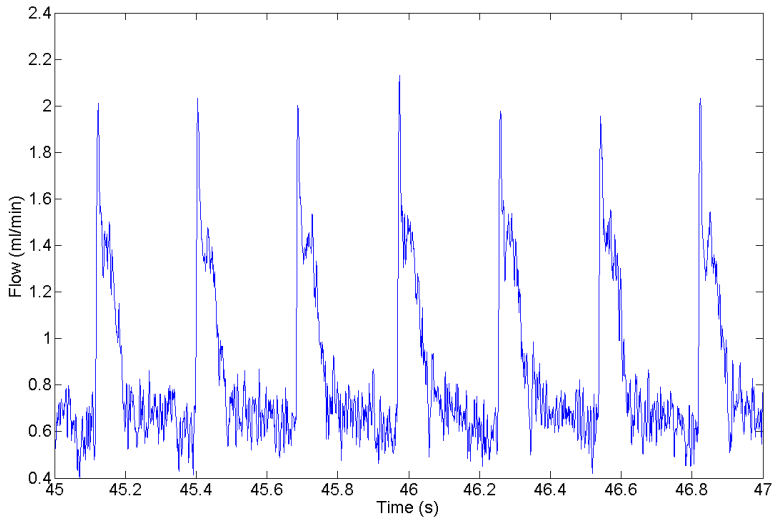


**Figure 9 - Mouse physiologic flow measure with Transit Time Ultrasound probe. Note the lower frequency (3.5 hz) due to the lower heart rate that results during sedation.**

At 1 Hz the system was able to produce physiologic, high flow, low-oscillatory, low, and sinusoidal waveforms at a steady pressure of 100mmhg. Also not that all graphs at 1 Hz do not include a +2 ml/min offset due zero flow calibration that was not performed. This offset is included for the graphs at 5 Hz and 10 Hz.

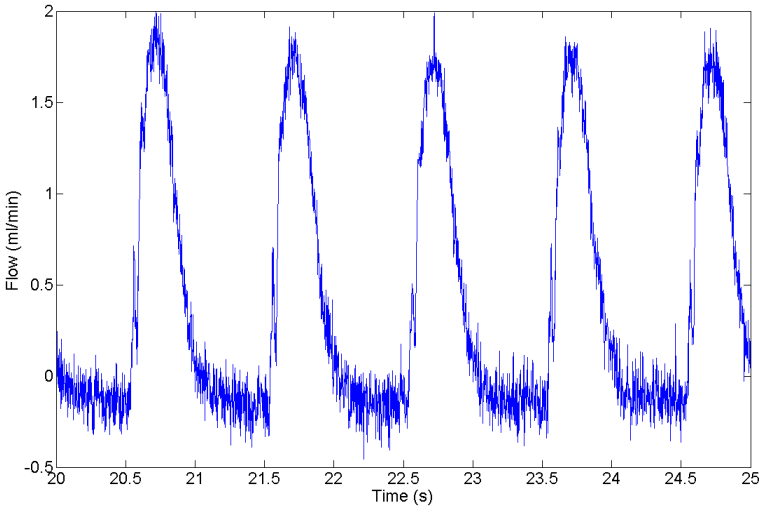


**Figure 10 – Physiologic waveform at 1 Hz and flow profile of [4, -2, 0, 0, 0]**

Note the max flow of 2.12 ml/min, the minimum flow of 0.18 ml/min, and mean flow of .62 ml/min. These values include a +2 ml/min offset. Although this physiologic mean flow is lower than the mean flow observed in the mouse this is often the benchmark mean flow rate for culturing murine carotid arteries[22]

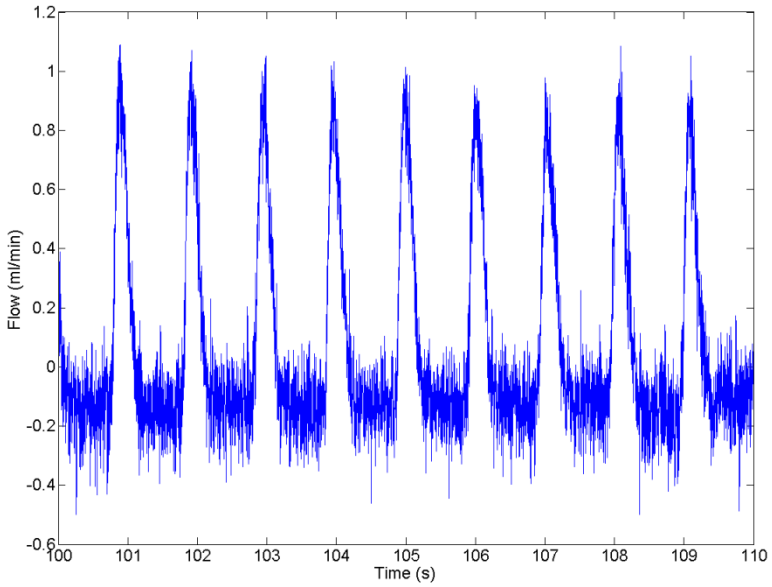


**Figure 11 – Low Flow waveform at 1 Hz with flow profile of [2, -1, -0.1, 0]**

The low flow waveform has a max flow of 1.05 ml/min, a minimum flow of -.07 ml/min, and a mean flow of .26 ml/min. Note the mean and max flow are half of the corresponding physiologic measurements.

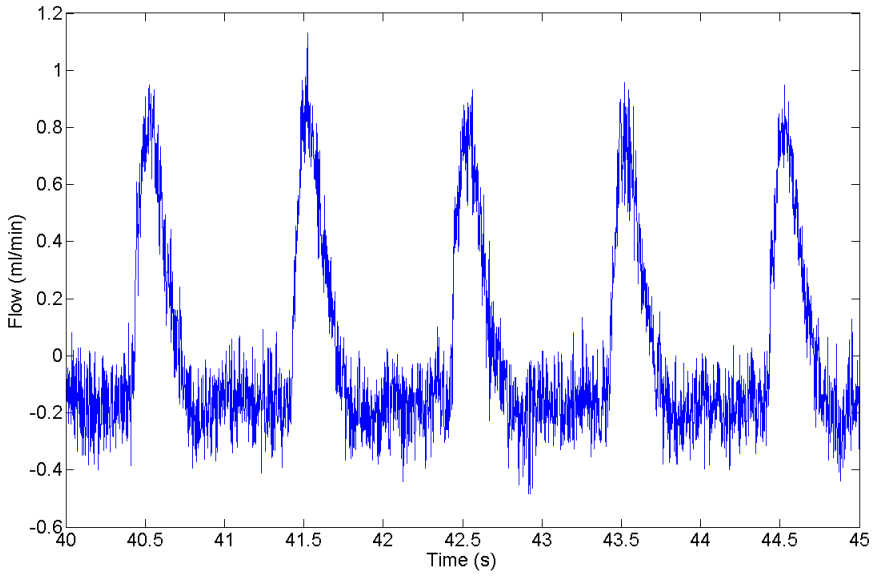


**Figure 12 –Low flow oscillatory waveform at 1 Hz with profile [2.8, -2, -0.1, -0.1, 0]**

The low-oscillatory waveform has similar properties to the low flow waveform but note the minimum flow of -.01 ml/min and the distinct oscillatory component that indicates reverse flow and also lowers the mean flow to .22 ml/min.

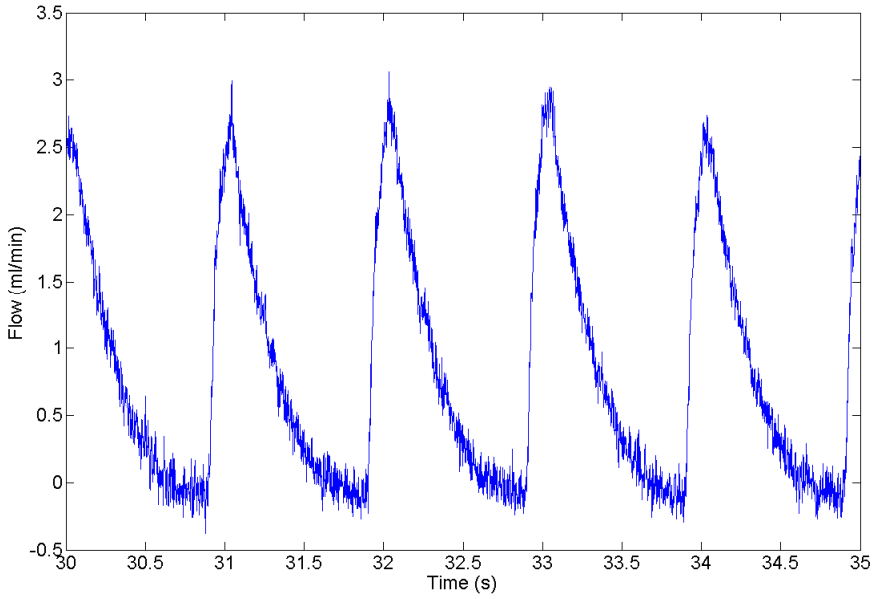


**Figure 13 – High flow waveform at 1 Hz with profile [12, -3, -0.1, 0, 0, 0, 0, 0, 0, 0]**

The high flow waveform has a maximum flow of 3.1 ml/min, a minimum flow of -.16 ml/min, and mean flow of 1.0 ml/min. The high flow not only results in higher shear stresses but also higher shear rates.

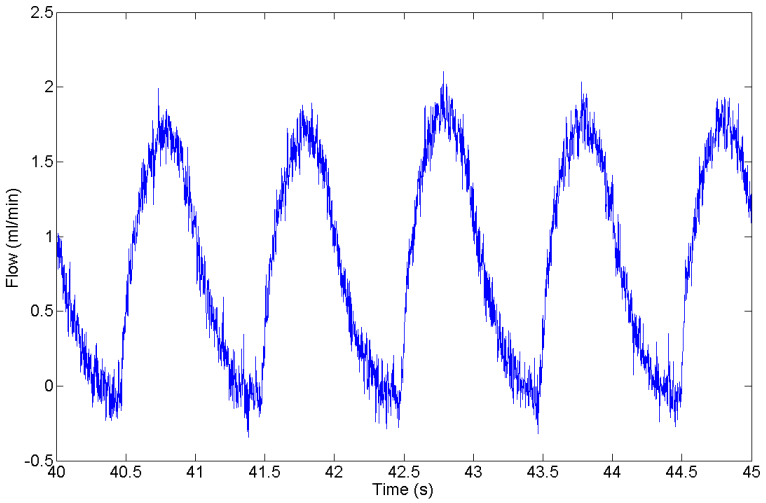


**Figure 14 - Sinusoidal waveform at 1 Hz with profile [3.75, -0.1, -0.1, 0]**

The sinusoidal waveform has similar maximum and minimum flows compared to the physiologic waveform. Not the lower flow rates and that result in lower shear rates due to shape of the waveform. This waveform also causes a slightly higher mean flow rate of 1.03 ml/min.

At 5 Hz the system was able to produce physiologic, physiologic-oscillatory, high flow, low-oscillatory, low, and sinusoidal waveforms at a steady pressure of 100mmhg. Note at all 5 Hz profiles have higher flow rates because of the shorter time course for each pulse. This results in higher flow rates and the resulting higher shear rates.

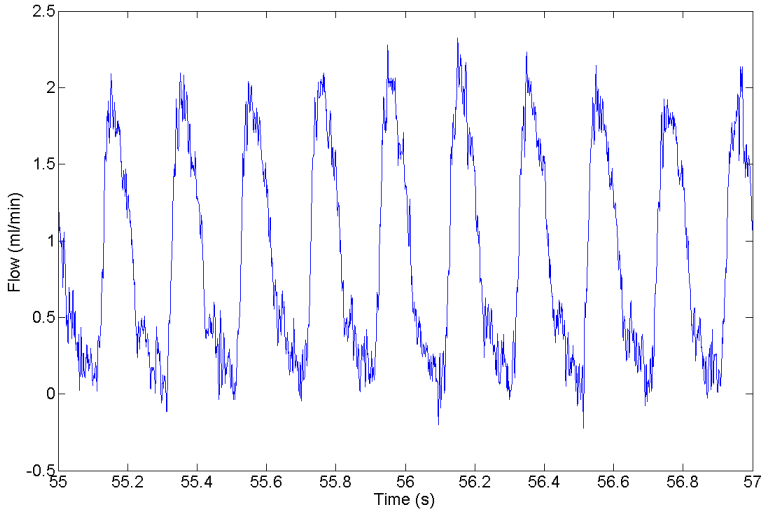


**Figure 15 - Physiologic waveform at 5 Hz with profile [9.5, -5, -.1, 0, 0]**

Note the max flow of 1.9 ml/min, the minimum flow of .01 ml/min, and mean flow of .86 ml/min. Although this physiologic mean flow is lower than the mean flow observed in the mouse this is often the benchmark mean flow rate for culturing murine carotid arteries

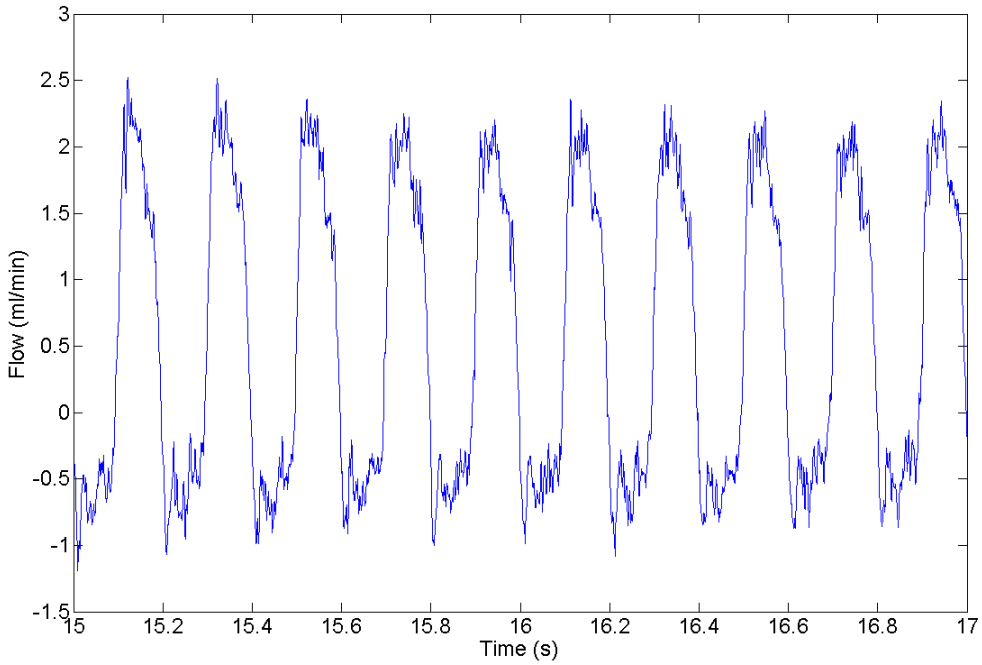


**Figure 16 - Physiologic-oscillatory waveform at 5 Hz with profile [15, -12, 0, 0, 0]**

This physiologic-oscillatory waveform is similar to the physiologic wave for with respect to shape and maximum flow. Note the minimum flow rate of -.41 ml/min and the mean flow of .79 ml/min

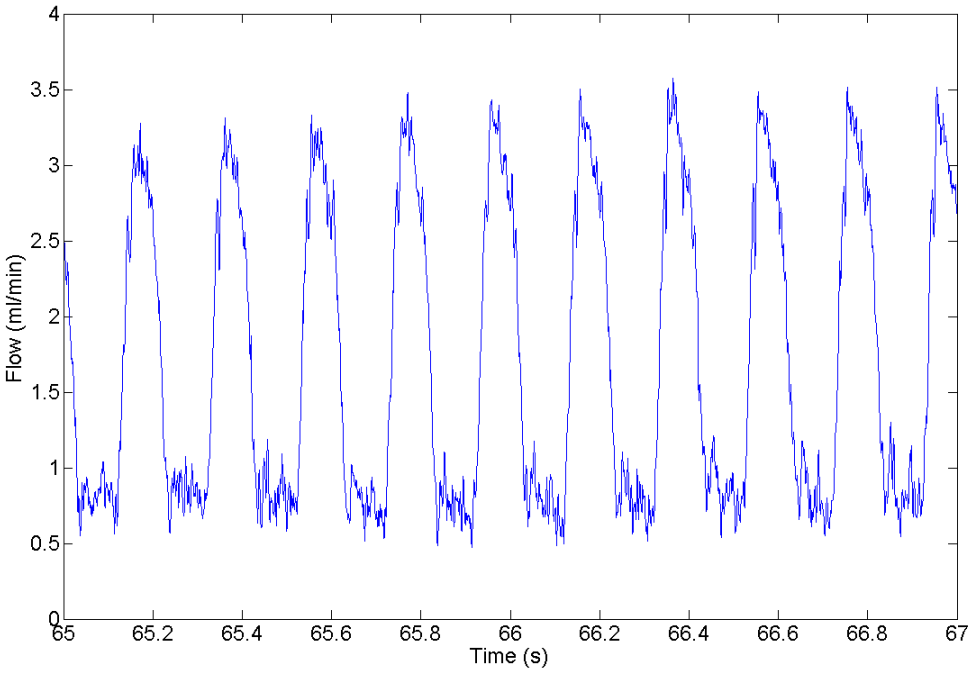


**Figure 17 - High flow waveform at 5 Hz with profile [14, -9, 0, 0, 0]**

The high flow waveform has maximum flow of 3.26 ml/min, a minimum flow of .67 ml/min and mean flow of 1.71 ml/min. At 5 Hz we begin to see the breakdown of the 1/3-2/3 pulsatile flow profile seen in the mouse. The profile here begins to look more sinusoidal when compare with a physiologic 1 Hz frequency or in-vivo profile, which reduces flow rates and in turn shear rates on endothelial cells.

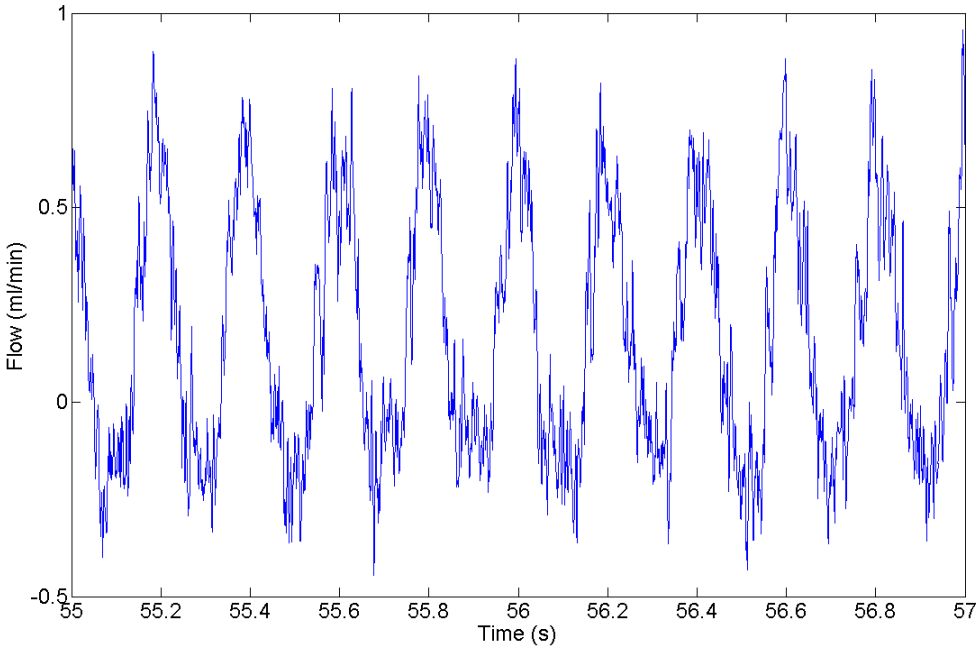


**Figure 18 - Low-oscillatory flow waveform at 5 Hz with profile [5, -3.75, 0, 0]**

The low–oscillatory flow waveform has a maximum flow of .79 ml/min and minimum flow of -.4 ml/min which gives the waveform its oscillatory component. The mean flow rate is .17 ml/min more the one half the mean flow rate of the physiologic mean flow rate.

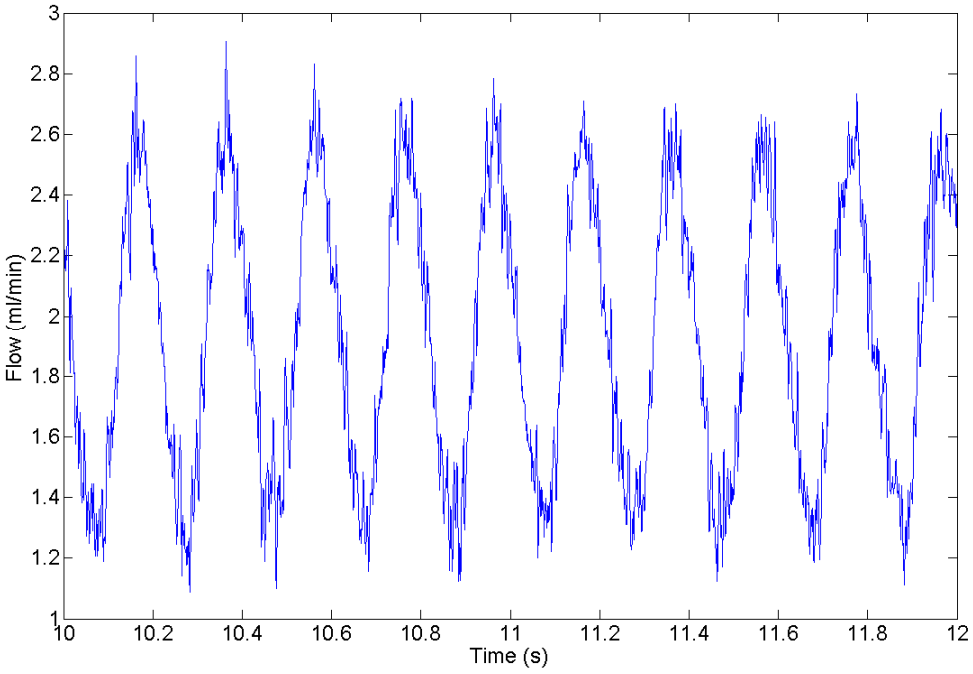


**Figure 19 - Sinusoidal flow waveform at 5 Hz with profile [1, 7.5, 1, -5, -0.1]**

The sinusoidal waveform at 5 Hz has a maximum flow of 2.7 ml/min and a minimum flow of 1.1 ml/min. Notice the lower flow rates that result from the sinusoidal waveform as compared to a physiologic waveform.

At 10 Hz the system was able to produce physiologic, physiologic-oscillatory, high flow, low-oscillatory, low, and sinusoidal waveforms at a steady pressure of 100mmhg.

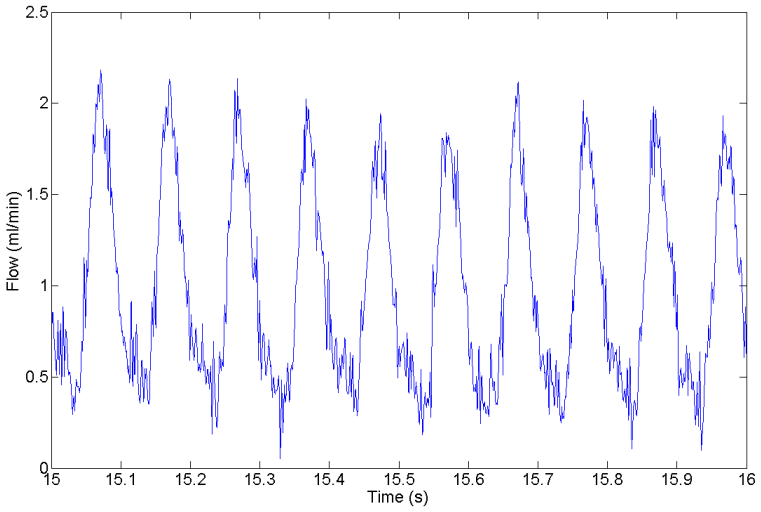


**Figure 20 - Physiologic waveform at 10 Hz with profile [11, -6, -0.5, 0, 0]**

The physiologic waveform at 10 Hz has a max flow of 1.87 ml/min and a minimum flow of .25 ml min with a mean flow of .98 ml/min. Notice that at this higher frequency the wave begins to look more sinusoidal resulting in lower than physiologic maximum shear rates.

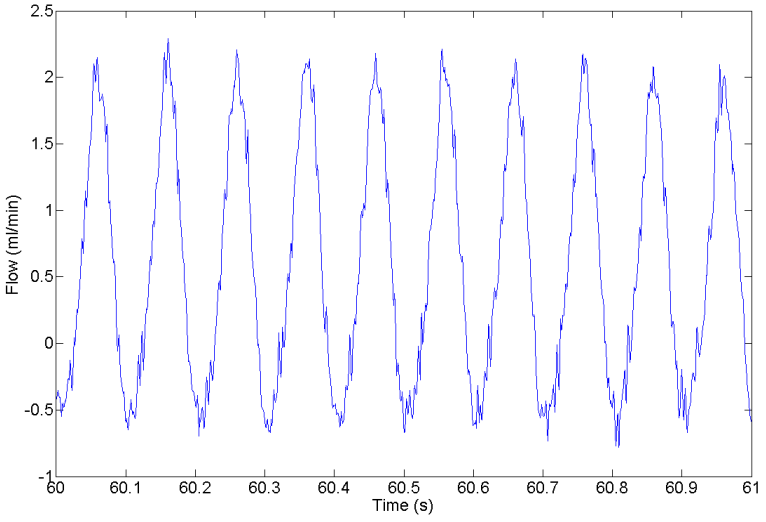


**Figure 21 - Physiologic oscillatory waveform at 10 Hz with profile [15, -12, 0, 0, 0]**

The physiologic-oscillatory waveform at 10 Hz has a maximum flow of 1.9 ml/min and a minimum flow of -.64 ml/min and a mean flow rate of .6 ml/min. Oscillating flow at this higher frequency appears to cause a more sinusoidal waveform, resulting in lower flow rates and in turn lower shear rates.

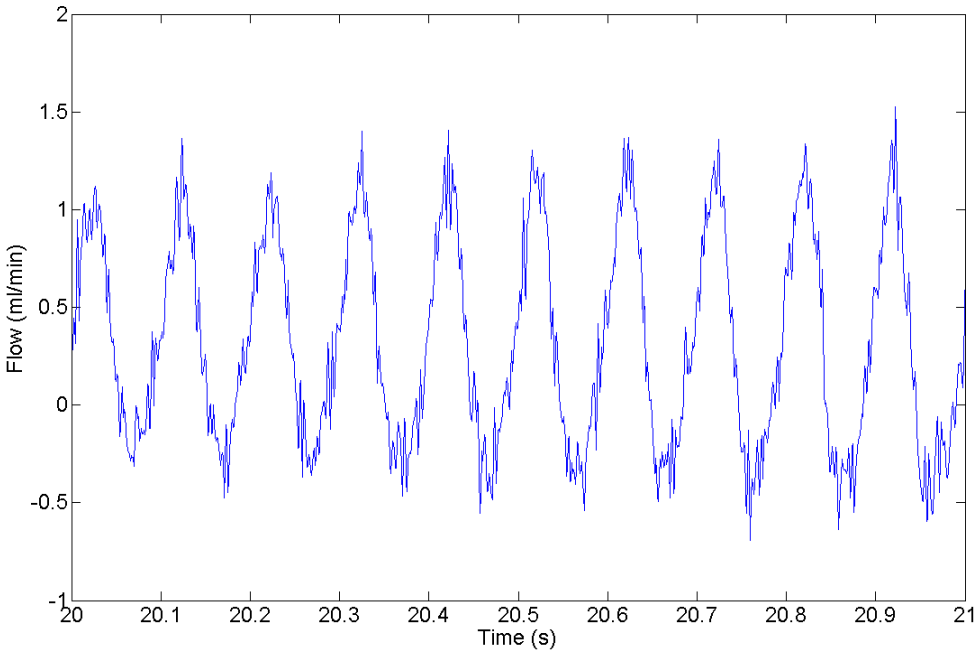


**Figure 22 – Low-oscillatory flow waveform at 10 Hz with profile [8.5--6—0]**

The low-oscillatory wave for has mean flow of .32 ml/min, a maximum flow of 1.34 ml/min, and a minimum flow of -.45 ml/min that gives the waveform its oscillatory component. Note the increased noise at the in the +/- .5 ml/min range. The sinusoidal affects on the waveform continue as seem with other oscillatory flows at this frequency. This noise effects result in lower flow-rates and in turn lower shear rates.

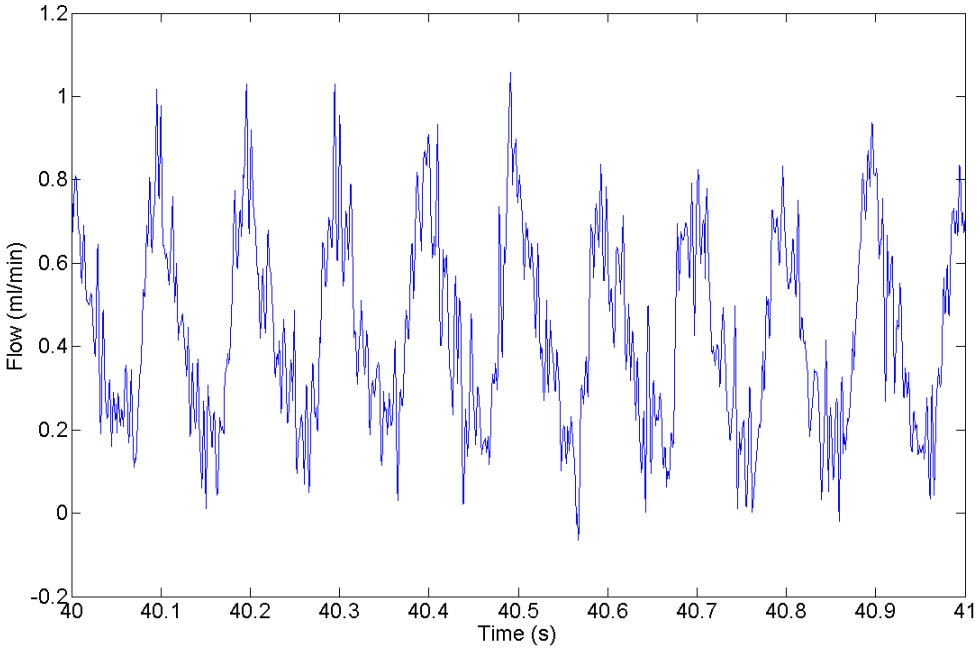


**Figure 23 - Low flow waveform at 10 Hz with profile [7.5, -4.5, 0]**

The low flow waveform at 10 Hz has a maximum flow rate of .94 ml/min, minimum flow rate of .07 ml/min, and a mean flow rate of .44 ml/min. Note that waveform has increased noise between .5 ml/min and 0 ml/min. Additionally the shape of the waveform resembles more of a saw tooth with the higher flow rates and corresponding shear rates that occur with physiologic flow at 10 Hz.

Shear stresses were calculated using the following estimation of wall shear stress.

$$\tau = 32uq/\pi d^3$$

Media with a viscosity of 1 cP was utilizes during the characterization of the system. In order to demonstrates the system's ability to perform with more viscous solution Dextran (6.5%) was added to the media to increase the viscosity to 4.2 cP which increases the wall shear stresses. The in-vivo shear stress on mouse carotid arteries is approximately

12 dynes/s. The 5 Hz and 10 Hz physiologic groups most closely achieve that shear level (~8 to 9.5 dynes/s). Shear levels for the all other groups are consistent between the 5 Hz and 10 Hz groups. Shear stress can be modulated in the future either by changing the viscosity, i.e. amount of Dextran, or the waveform.

| | | | Diameter(cm) | 0.056 | | | media viscosity(cP) | 1 | | | media w/dextran viscosity (cP) | 4.2 | |
|---|---|---|---|---|---|---|---|---|---|---|---|---|---|
| Frequency (Hz) | Waveform | | mean flow (ml/min) | min flow (ml/min) | max flow (ml/min) | | mean wss (dynes/s) | min wss (dynes/s) | max wss (dynes/s) | | mean wss (dynes/s) | min wss (dynes/s) | max wss (dynes/s) |
| 1 | phys | | 0.62 | 0.18 | 2.12 | | 5.99 | 1.74 | 20.49 | | 25.17 | 7.31 | 86.07 |
| 1 | low-osc | | 0.2216 | -0.01 | 0.42 | | 2.14 | -0.10 | 4.06 | | 9.00 | -0.41 | 17.05 |
| 1 | low | | 0.264 | -0.07 | 1.05 | | 2.55 | -0.68 | 10.15 | | 10.72 | -2.84 | 42.63 |
| 1 | high | | 1.018 | -0.16 | 3.08 | | 9.84 | -1.55 | 29.77 | | 41.33 | -6.50 | 125.05 |
| 1 | sine | | 1.03 | -0.08 | 2.26 | | 9.96 | -0.77 | 21.85 | | 41.82 | -3.25 | 91.76 |
| 5 | phys | | 0.86 | 0.01 | 1.9 | | 8.31 | 0.10 | 18.37 | | 34.92 | 0.41 | 77.14 |
| 5 | low-osc | | 0.17 | -0.41 | 0.79 | | 1.64 | -3.96 | 7.64 | | 6.90 | -16.65 | 32.07 |
| 5 | low | | 0.34 | -0.05 | 0.82 | | 3.29 | -0.48 | 7.93 | | 13.80 | -2.03 | 33.29 |
| 5 | high | | 1.71 | 0.67 | 3.26 | | 16.53 | 6.48 | 31.51 | | 69.43 | 27.20 | 132.36 |
| 5 | sine | | 1.93 | 1.11 | 2.7 | | 18.66 | 10.73 | 26.10 | | 78.36 | 45.07 | 109.62 |
| 5 | phys-osc | | 0.53 | -0.78 | 2.2 | | 5.12 | -7.54 | 21.27 | | 21.52 | -31.67 | 89.32 |
| 10 | phys | | 0.98 | 0.25 | 1.87 | | 9.47 | 2.42 | 18.08 | | 39.79 | 10.15 | 75.92 |
| 10 | low-osc | | 0.32 | -0.45 | 1.34 | | 3.09 | -4.35 | 12.95 | | 12.99 | -18.27 | 54.41 |
| 10 | low | | 0.44 | 0.07 | 0.94 | | 4.25 | 0.68 | 9.09 | | 17.86 | 2.84 | 38.16 |
| 10 | phys-osc | | 0.6 | -0.64 | 1.9 | | 5.80 | -6.19 | 18.37 | | 24.36 | -25.98 | 77.14 |

**Figure 24 - Mean, Maximum, and Minimum Shear Stresses and Flows at 1 Hz, 5 Hz, 10 Hz**

## *Cell Viability*

### MTT Assay

Both the control vessel and cultured vessel turned purple after exposure to the MTT assay (Figure 22). However the cultured vessel was noticeably purple in the lumen of the vessel (Figure 22B) while the control vessel that was noticeably purple in lumen and adventitia (Figure 22A). Both arteries were segmented before introduction into the MTT assay however only one segment was analyzed from the experimental group as suture segments adhered to the remainder of the vessel, causing those segments to appear darker and purple.

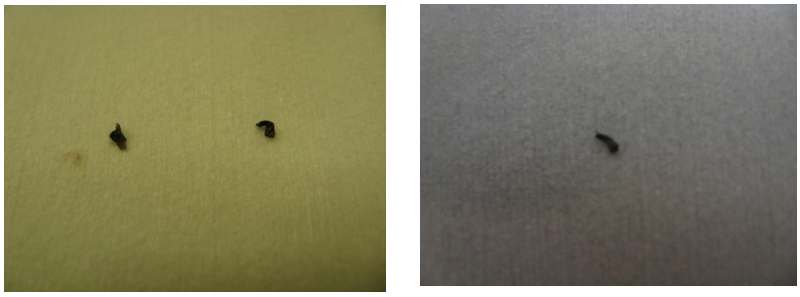

A B

**Figure 25 - A) Control vessel freshly isolated and exposed to MTT. B) Vessel after 6 hours of culture with physiologic waveform at 10 Hz.**

## Functional Testing

After 6 hours of culture under physiologic waveform at 10 Hz the addition of PE ($10^{-5}$M) did not result in vessel constriction within 20 minutes. The addition of ACh ($10^{-5}$) did not result in vessel dilation or constriction after 20 minutes and the addition of SNP ($10^{-4}$) did not show any additional dilation.

## *Nitric Oxide Production*

NO release was measured while culturing the vessel with a 10 Hz physiologic waveform. The results are shown in figure 22. The vessel is held at static flow time 50s when media begins to flow through the vessel at physiologic conditions. NO release peaks at 100s and appears to reach its steady state 225s; however small local peak occur in NO while at steady state. This is most likely due to the zero flow that occurs while the motor transitions from one direction to the other; the NO level appears to return to its steady state level.

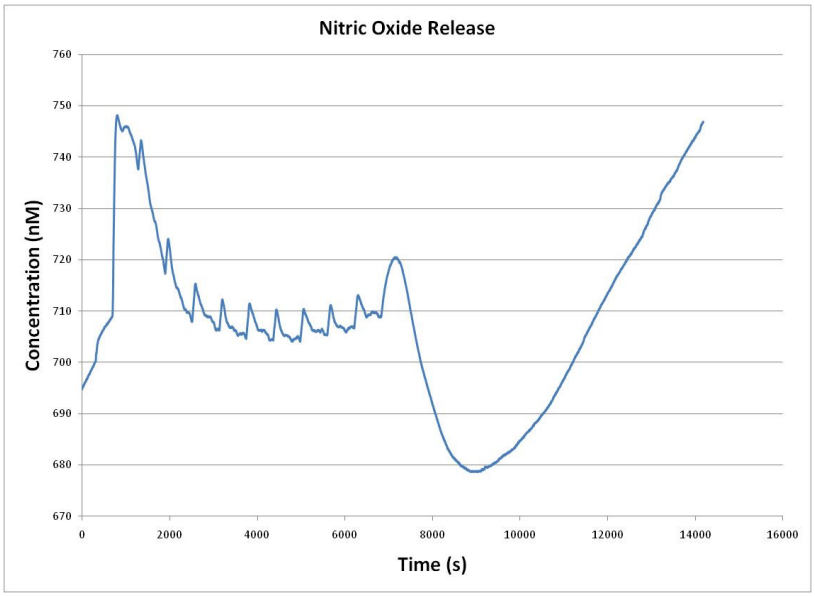


**Figure 26 - This figure shows the concentration of NO measure distal to the vessel. The vessel is cultured under static conditions. At 50 s, where the sharp peak is observed, physiologic culture was started at 10 Hz. This is followed by a precipitous increase in NO concentration until 100 s when the NO concentration decreases until it stabilizes at approximately 705 nM. Flow is terminated at 675 s**

## *Reactive Oxygen Species Production*

Increased expression of ROS is clearly evident in the positive control group; vessels treated with LPS, as compared to the freshly isolated group. Differences in ROS expression were not evident when comparing images of a vessel cultured at low flow with one cultured at physiologic flow. Additionally differences in ROS expression were difficult to assess in images taken before and after introducing a vessel to the ROS probe.

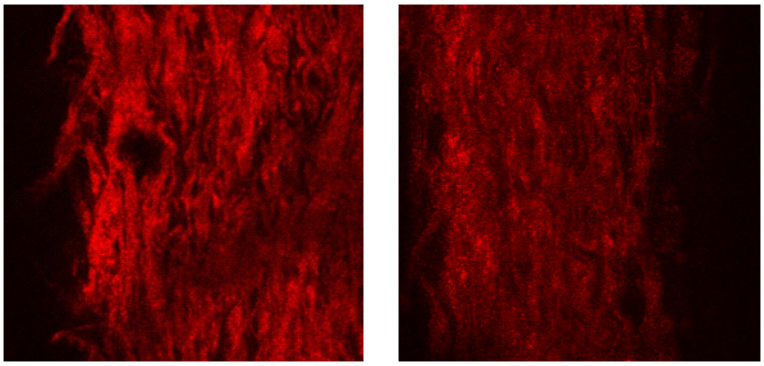

A B

**Figure 27 - Images of same carotid artery after 6 hour culture while mounted on device. A) Before introduction of HCy3 ROS probe B) After introduction of HCy3 ROS probe. After introducing the probe into the lumen of the vessel no significant fluorescence is visible.**

## *Discussion*

With this study we were able to show the devices capability to modulate the shape of the waveform by changing the max flow, minimum flow, directions of flow, or shape of flow profile at various frequencies. However this ability diminishes as frequency increases. This resulted in more sinusoidal waveforms that don't produce the higher shear rates of physiologic waveforms. Additionally we were able to monitor diameter, flow, pressure, NO in real-time, and possibly ROS if expression techniques can be developed to image for HCy3 without having to fix cells. This device is able to test acute, intermediate, and long term effect on remodeling and morphogenesis of changes to any global or local parameter that is flow depending(mean flow, max flow, oscillatory flow, flow rate, shear stress). This includes short term culture (6 hours), intermediate culture (1-2 days), and long term culture (1-2 weeks)

System performance was excellent with no seizing of the motor or contamination within the 6 hour culture. Occasionally distilled water was dropped on the syringe shafts during testing to increase lubrication within the syringe.

Flow rates in the range of +/- . 5ml/min were difficult to quantify because of electrical noise in the system. This was especially apparent when placing the entire system within the incubator. All experiment were conducted using DMEM with have approximately 1/3 the viscosity of blood. In order to test any hypothesis using oscillatory waveforms it is recommended that the viscosity remain low so as to decrease the shear

stress. This allows for the use of higher flow to achieve desired in-vivo shear rate and avoid the noise complications and compressibility issues seen at low oscillating flow rates of the system. De-gassing the liquid used may allow for accurate measurements of flow in the +/- 5 ml/min range as the fluid would become more incompressible resulting in a quicker response to changes in direction.

During functional testing the mitochondrial activity was evident in both the control and experimental vessel. The experimental vessel only showed evidence of mitochondrial activity in the lumen suggesting that cells in the adventitia and the outside of the vessel had died while endothelial and smooth muscle cells remained viable. Functional testing of endothelial and smooth muscle cell functionality was not successful despite the presence of mitochondrial activity in those areas. Functional testing has worked previously on the device under less physiologic flow conditions therefore it is unclear why the SMCs and EC did not respond to their respective stimuli.

The acute NO release during short no flow changes is an interesting phenomena. That requires further investigation. Because of NO's atheroprotective nature it would be expected to have higher concentration at higher flows, not lower flows. Additional the NO concentration levels were testes after depressurizing the vessel because the using the probe under pressure without clamping down on the probe body caused media to leak inside the probe causing it read it maximum value.

We were able to see increase in ROS expression when using a positive control. Unfortunately now significant differences in fluorescence were visible after culture with low flow compared to physiologic flow. Refinements in confocal microscopy techniques may be necessary in order to track these differences in ROS expression. Additionally

opening up the vessel en face may give a better window to look at the cells and determine ROS expression. However this method would prevent the observation of real-time production of ROS which can be accomplished via mounting the Living Systems device on the confocal microscopy while culturing with media infused with HCy3.

## *Limitations and Future Work*

With the current set-up the pulse pressure remains static during culture. The addition of a second linear motor in series with the pressure transducers as seen below in figure 28 should give the system the ability to impose pulse pressure of different magnitudes as well as vary the timing of the pulse pressures. This allows for the pulse pressure to be in or out of face with the pulsatile flow.

In order to accomplish longer cultures of 1 to 2 weeks, an enclosure may be necessary for the motor and syringes in order to prevent contamination of the media via the syringe shafts that are open to the air during their draw cycle.

A more exhaustive analysis of the flow conditions near the wall would be necessary to determine more accurately shear stresses acting near the wall on the endothelial cells. This could be achieved using and oscillatory index or other numerical analysis[8].

A system that uses Fourier series to fit the flow waveform produced to a desired flow waveform would significantly reduce the time currently required to do this iteration manually. With the current system the operator must read each waveform from the flow data of the ultrasound probe and make adjustment manually to the motor motion to try and fit the actual curve to the desired curve. The development of each curve can take upwards of two hours.

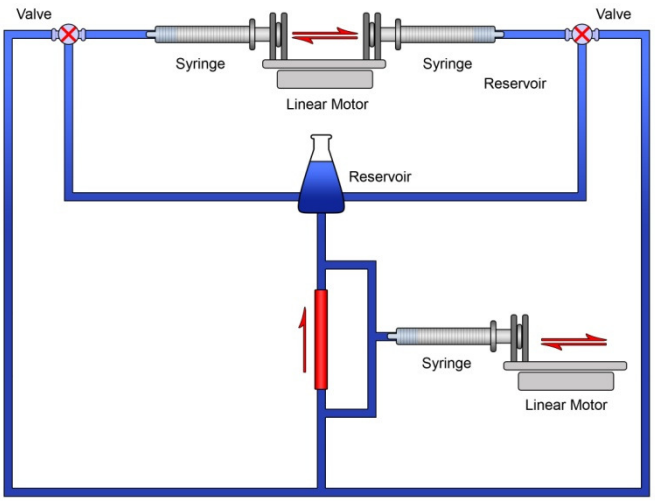


**Figure 28 - Future Design to Incorporate Pulse Pressure**

# CHAPTER 5: CONCLUSIONS

A novel device was developed to study the effects of a wide range of flow conditions on extracted mouse carotid arteries. A number of designs were considered with the final design incorporating a computer controlled linear motor that drives two syringes in opposite direction with two computer controlled valve that assures forward flow through the vessel. Additionally the device integrated a camera, pressure transducers, and flow meter in order to monitor this information in real-time. All electromechanical parts of the system were integrated using a comprehensive Labview code.

The device was successful at producing physiologic, high, low, low-oscillatory, sinusoidal flow waveforms at frequencies ranging from 1 to 10 Hz; additionally the device it able to produce these waveforms at very low flows, +/- 3 ml/min. Shear stresses experienced by endothelial cells on the vessel mounted in the system can be modulated either by changing the viscosity of the liquid or changing the waveform of the flow through the vesse

Real-time NO detection was successfully integrated into the system via use a computer integrated probe. Changes in NO release were detected when changing to flow from static conditions to physiologic and vice versa. ROS detection wproved more difficult as no discernable difference was seen between the vessels cultured under low flow conditions and physiologic flow conditions. However improved confocal microscopy techniques may reveal more discernable results.

# APPENDIX A: MATLAB CODE TO DISCRETIZE FLOW

```
clear
clc
freq = input('What Frequency (Hz) ')
points = input('How many discretized points of the flow profile ')
dt = (1/freq)/points;

draw_length = 58.9;  %in mm
draw_volume = 1.0; % in mL
conversion = (1/60)*(draw_length/draw_volume); %conversion of mL/min to
mm/s
max_length = 20; % longest travel possible without causing a fault
30max

%enter flow profile points
title_prof =''
for i=1:points
flow_prof(i) = input('Enter point value ')
title_prof = strcat(title_prof,num2str(flow_prof(i)),'-')
end

%make flow profile into string

%initial conditions
time(1) = 0;
int_flow(1) = 0;
i = 2;
count = 1;
xposition(1) = 0;

flow_prof(points+1) = flow_prof(1);

%forward movement
while max(xposition) < max_length
    time(i) = time(i-1) + dt;
    int_flow(i) = ((flow_prof(count) + flow_prof(count+1))/2) * dt *
conversion;
    xposition(i) = (int_flow(i) + xposition(i-1));
    if count == points
        count = 1;
    else
        count = count + 1;
    end
    i = i + 1;
end



while min(xposition) >= -1
    time(i) = time(i-1) + dt;
    int_flow(i) = ((flow_prof(count) + flow_prof(count+1))/2) * dt *
conversion;
    xposition(i) = (xposition(i-1) - int_flow(i));
    if count == points
```

```
        count = 1;
    else
        count = count + 1;
    end
       i = i + 1;
end
fp = fopen(sprintf('Frequency=%d(Hz)_Points=%d_Profile=%s', freq,
points, title_prof), 'w');

for i=1:length(xposition)
         fprintf(fp,sprintf('k %.3f x %.3f\n', time(i), -
xposition(i)));
end
```

# APPENDIX B: MATLAB CODE TO PROCESS FLOW DATA

```
clc
clear all;
close all;

Start_Path = 'C:\Documents and Settings\Lab\My Documents\Seth\flow
data\*.*';
[Raw_File,fPath] = uigetfile(Start_Path,'Select any file in the correct
directory');

file=strcat(fPath,Raw_File);
flow_data = load(file);

%determine time increment
raw_time = flow_data(:,1);
count = 0;
start = 0;
status = 0;

%determine when time starts
for i=1:length(raw_time)-1
    while (status == 0)&& (raw_time(i+1,1)~= raw_time(i,1))
        start = i;
        status = 1;
    end
end

%determine when time stops
status2 = 0;
stop = 0;
for i=start+1:length(raw_time)-1
    while (status2 == 0)&& (raw_time(i+1,1)~= raw_time(i,1))
        stop = i;
        status2 = 1;
    end
end

%construct time array
time_inc = 1/(stop-start);
time = linspace (0,length(raw_time),length(raw_time))*time_inc;
time = time';

%process flow data
raw_flow = flow_data(:,2);
proc_flow = (raw_flow*2.5)/(1000);

all_data = [time proc_flow];


%plot flow profile
figure(1)
set(gca,'Fontsize',18)
plot(time,proc_flow,'LineWidth',.1)
```

```
title(Raw_File);
xlabel('Time (s)');ylabel('Flow (ml/min)');
fPath=strcat(fPath,'analysis\',Raw_File,'.png');
saveas(1,fPath,'png');

% %determine mean flow rate
% start_flow = input('When does flow begin?');
% stop_flow = input ('When does flow cease?');
%
%
% proc_flow_trimmed =
proc_flow((start_flow/time_inc):(stop_flow/time_inc)
% mean_flowrate = mean(proc_flow_trimmed)
```

# APPENDIX C: LABVIEW CODE TO CONTROL SYSTEM

Connector Pane

**Seth Mouse System pressure diameter.vi**

---

Front Panel

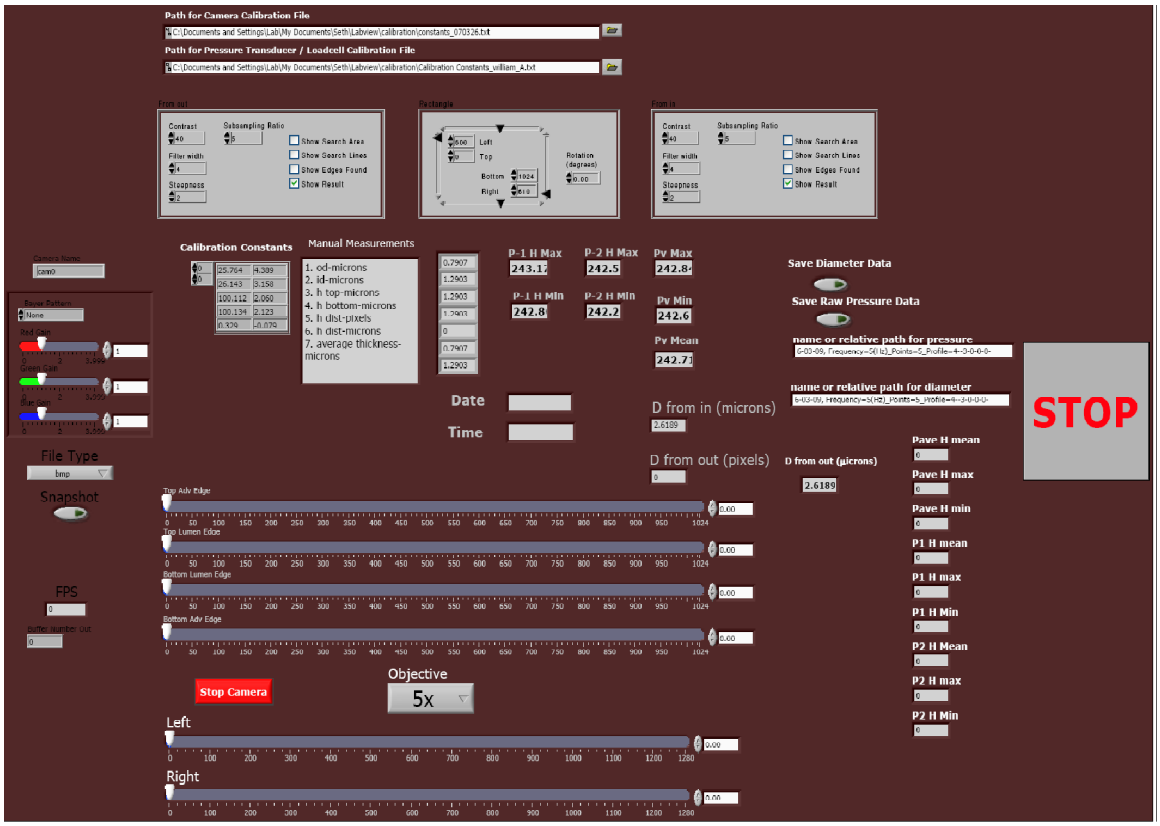

Block Diagram

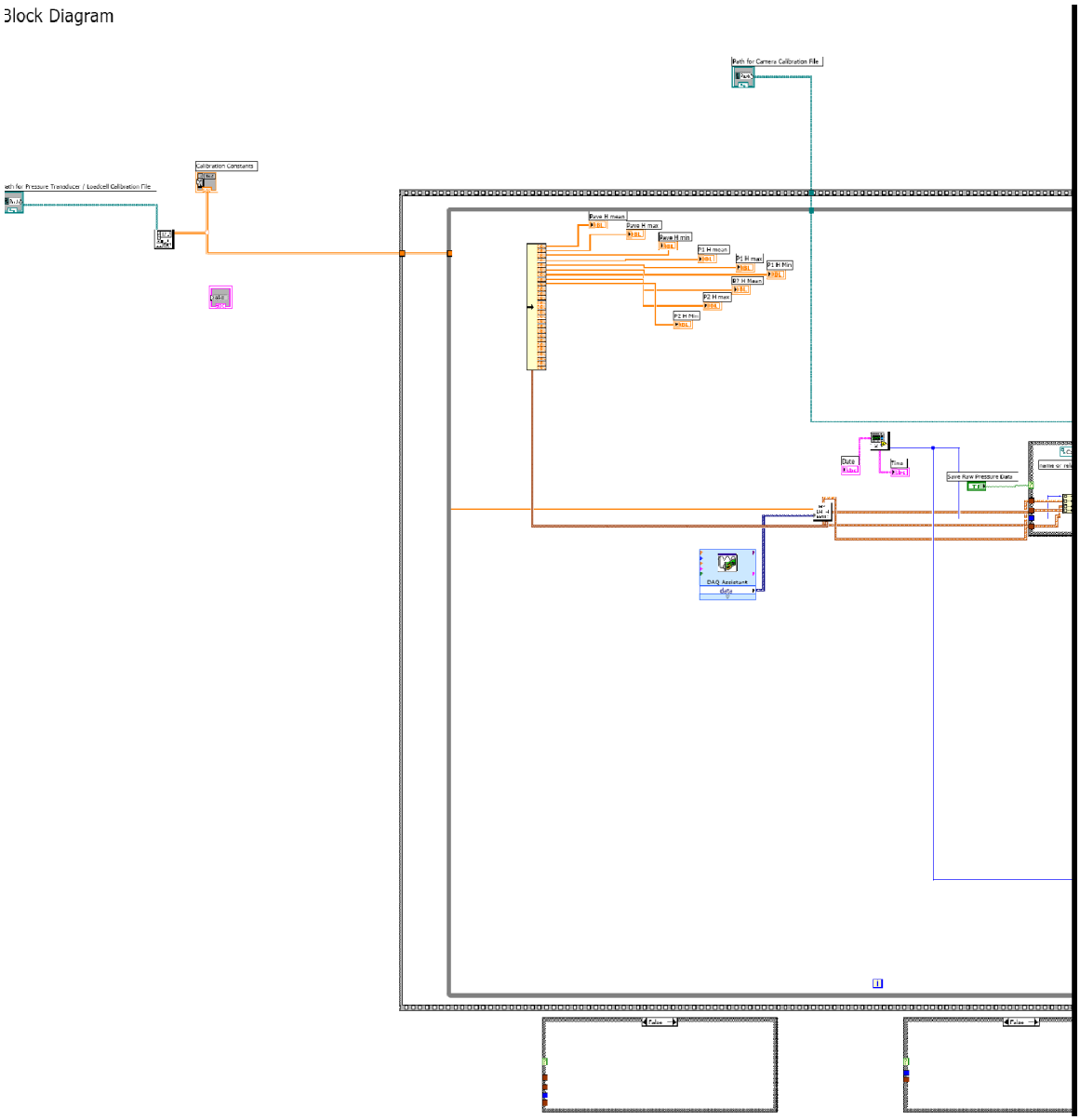

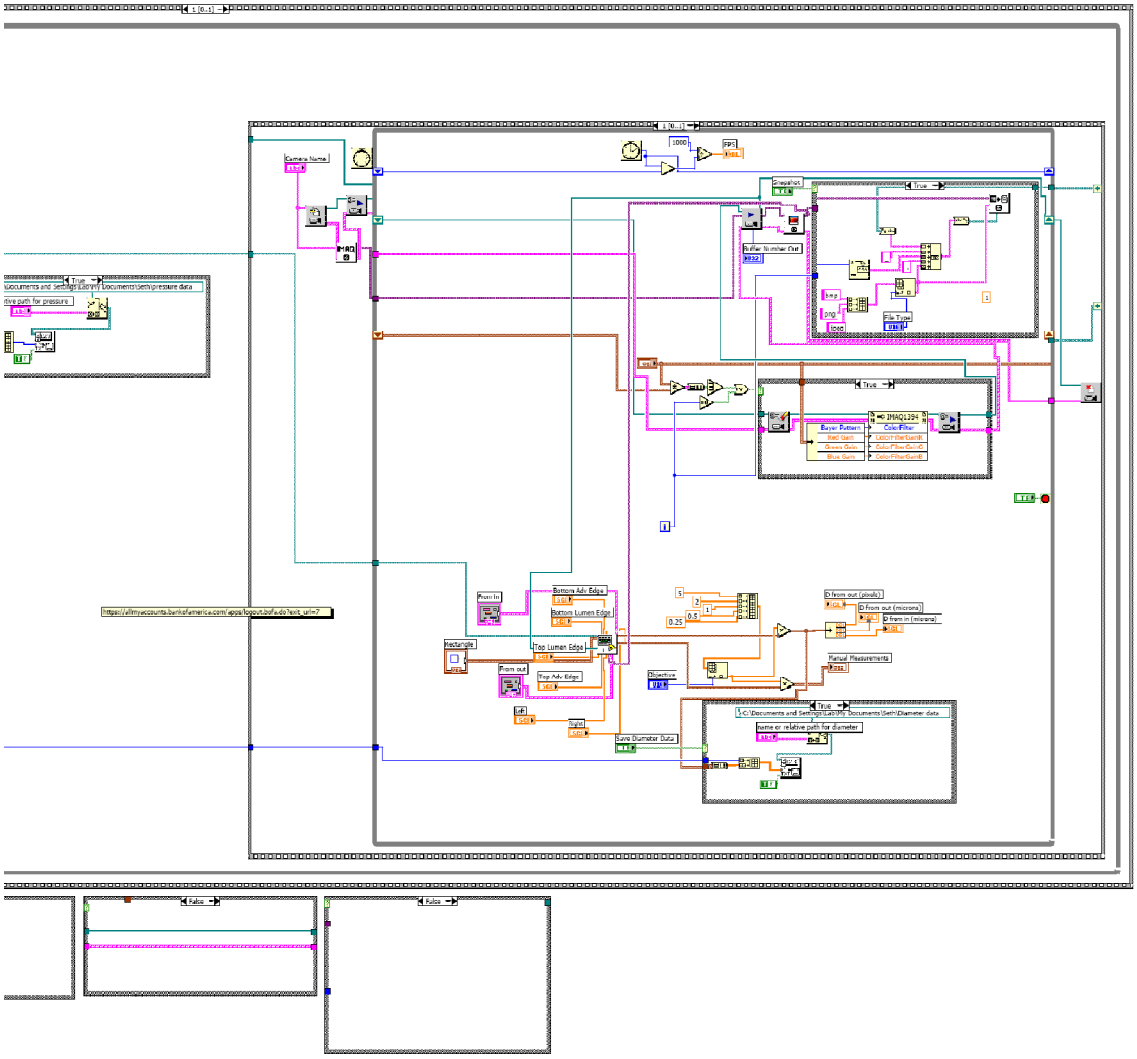
Camera Name
FPS
Snapshot
Buffer to mhar Out
File Type
Bayer Pattern
Red Gain
Green Gain
Blue Gain
Bottom Adv. Edge
Bottom Lumen Edge
Top Lumen Edge
Top Adv. Edge
From out
Rectangle
Objective
Natural Measurements
Save Diameter Data
Name or relative path for diameter
D from out (pixels)
D from out (microns)
D from in (microns)
False
False

## *REFERENCES*


1. WRITING GROUP MEMBERS, et al., *Heart Disease and Stroke Statistics--2009 Update: A Report From the American Heart Association Statistics Committee and Stroke Statistics Subcommittee.* Circulation, 2009. **119**(3): p. e21-181.

2. Humphrey, J.D., ed. *Cardiovascular Solid Mechanics: Cells, Tissues, and Organs*. 2002, Springer: New York.

3. Ku, D.N., *BLOOD FLOW IN ARTERIES.* Annual Review of Fluid Mechanics, 1997. **29**(1): p. 399-434.

4. Matsumoto, T. and K. Hayashi, *Stress and Strain Distribution in Hypertensive and Normotensive Rat Aorta Considering Residual Strain.* Journal of Biomechanical Engineering, 1996. **118**(1): p. 62-73.

5. Kamiya, A. and T. Togawa, *Adaptive regulation of wall shear stress to flow change in the canine carotid artery.* Am J Physiol Heart Circ Physiol, 1980. **239**(1): p. H14-21.

6. Jackson, Z.S., A.I. Gotlieb, and B.L. Langille, *Wall Tissue Remodeling Regulates Longitudinal Tension in Arteries.* Circ Res, 2002. **90**(8): p. 918-925.

7. Masuda, H., et al., *Adaptive Remodeling of Internal Elastic Lamina and Endothelial Lining During Flow-Induced Arterial Enlargement.* Arterioscler Thromb Vasc Biol, 1999. **19**(10): p. 2298-2307.

8. Ku, D., et al., *Pulsatile flow and atherosclerosis in the human carotid bifurcation. Positive correlation between plaque location and low oscillating shear stress.* Arterioscler Thromb Vasc Biol, 1985. **5**(3): p. 293-302.

9. Zarins, C., et al., *Carotid bifurcation atherosclerosis. Quantitative correlation of plaque localization with flow velocity profiles and wall shear stress.* Circ Res, 1983. **53**(4): p. 502-514.

10. Giddens, D.P., C.K. Zarins, and S. Glagov, *The Role of Fluid Mechanics in the Localization and Detection of Atherosclerosis.* Journal of Biomechanical Engineering, 1993. **115**(4B): p. 588-594.

11. Vinay Kumar, A.K.A., Nelson Fausto and Richard Mitchell, *ROBBINS BASIC PATHOLOGY*. 7 Sub edition ed. Vol. . 2007: W.B. Saunders Company. 960.

12. Griendling, K.K., D. Sorescu, and M. Ushio-Fukai, *NAD(P)H Oxidase : Role in Cardiovascular Biology and Disease.* Circ Res, 2000. **86**(5): p. 494-501.

13. Forstermann, U. and T. Munzel, *Endothelial Nitric Oxide Synthase in Vascular Disease: From Marvel to Menace.* Circulation, 2006. **113**(13): p. 1708-1714.

14. Forstermann, U., et al., *Nitric oxide synthase isozymes. Characterization, purification, molecular cloning, and functions.* Hypertension, 1994. **23**(6): p. 1121-1131.

15. Abilez, O., et al., *A Novel Culture System Shows that Stem Cells Can be Grown in 3D and Under Physiologic Pulsatile Conditions for Tissue Engineering of Vascular Grafts.* Journal of Surgical Research, 2006. **132**(2): p. 170-178.

16. Gleason, R.L., et al., *A Multiaxial Computer-Controlled Organ Culture and Biomechanical Device for Mouse Carotid Arteries.* Journal of Biomechanical Engineering, 2004. **126**(6): p. 787-795.

17. Peng, X., et al., *In vitro system to study realistic pulsatile flow and stretch signaling in cultured vascular cells.* Am J Physiol Cell Physiol, 2000. **279**(3): p. C797-805.

18. James E. Moore Jr. Contact Information, E.B., Andreas Suciu, Shumin Zhao, Michel Burnier, Hans R. Brunner and Jean-Jacques Meister, *A device for subjecting vascular endothelial cells to both fluid shear stress and circumferential cyclic stretch.* Annals of Biomedical Engineering, 1994. **22**(4): p. 6.

19. Janssen, B.J.A., P.J.A. Leenders, and J.F.M. Smits, *Short-term and long-term blood pressure and heart rate variability in the mouse.* Am J Physiol Regul Integr Comp Physiol, 2000. **278**(1): p. R215-225.

20. Conway, D.E., et al., *Expression of CYP1A1 and CYP1B1 in human endothelial cells: regulation by fluid shear stress.* Cardiovasc Res, 2009. **81**(4): p. 669-677.

21. Kousik Kundu, et al., *Hydrocyanines: A Class of Fluorescent Sensors That Can Image Reactive Oxygen Species in Cell Culture, Tissue, and In Vivo13.* Angewandte Chemie International Edition, 2009. **48**(2): p. 299-303.

22. Transonic Systems, I., *Tools and Techniques for Hemodynamic Studies in Mice* Available at http://www.transonic.com., 1997.